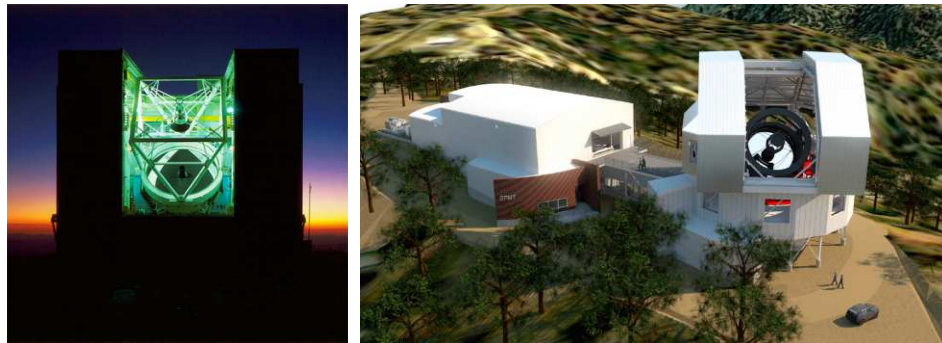# PROPOSED SCIENCE CASES FOR A JOINT
MEXICO-USA OBSERVATORY:

MMT TELESCOPE
(SMITHSONIAN, U. ARIZONA)

AND

TELESCOPIO SAN PEDRO MARTIR (TSPM)

July 2015

Edited by

Luis Corral Escobedo
Instituto de Astronomía, Universidad de Guadalajara

Teresa García Díaz
Instituto de Astronomía, Ensenada-UNAM

Fernando Fabián Rosales Ortega
Instituto Nacional de Astrofísica Óptica y Electrónica

Alan Watson
Instituto de Astronomía, CU-UNAM

Foreword

A foreword must be included?

Lorem ipsum dolor sit amet, consectetur adipiscing elit. Quisque sodales tincidunt purus id iaculis. Nulla sagittis ut magna quis lacinia. Fusce ullamcorper, massa interdum molestie accumsan, ipsum velit bibendum erat, non bibendum odio felis suscipit ipsum. Quisque nec tristique libero. Aliquam vel felis gravida, tincidunt ex in, porttitor ligula. Integer at urna egestas, ornare mauris et, lobortis tellus. Sed sagittis sollicitudin eleifend. Praesent mollis erat ante, id fermentum ex gravida sed. Cras eget nunc vel magna consectetur rhoncus. Integer non neque augue.

Someone here, many the Head of some Institute
Somewhere in México D.F., July 2015

Contents

Part III   Cosmology

Part IV   Future Instrumentation

Part I
Galactic and stellar astronomy

Chromospheric activity and age of solar analogs in open clusters

EMANUELE BERTONE AND MIGUEL CHÁVEZ

Instituto Nacional de Astrofísica, Óptica y Electrónica
Luis Enrique Erro 1, Tonantzintla, Puebla, México

INSTRUMENT: HECTOCHELLE

1 Introduction

Open clusters represent a most valuable laboratory for understanding the physics of stars. Having a common origin, member stars are usually considered coeval and initially chemically homogeneous. The age of the cluster can be therefore easily and quite precisely obtained (once the chemical abundances are known) by isochrone fitting.

On the contrary, age determination methods for field stars are usually affected by larger uncertainties (see, for instance, the excellent review on this topic by Soderblom 2010). For this reason, stars in clusters are excellent targets to calibrate the connection between age and age-dependent stellar properties, correlations which can be eventually applied to field stars.

In this context, Hectochelle, with its multi-object capability coupled to the large collecting area of a 6.5 m telescope, represents a ideal instrument for the study of the resolved stellar population of Galactic stellar clusters: it will efficiently gather high-quality spectra of fainter stars in the CMD diagrams of more distant objects (the lower-resolution Binospec spectrograph can be also useful for fainter and younger clusters, where the Ca HK lines presumably are more intense). As we shall see below, observations of main sequence (MS) stars will be feasible on systems up to several kiloparsecs.

Of particular interest is the study of solar analogs. In fact, the discovery of hundreds of extrasolar planets in the recent years has renewed the interest of the astrophysical community on solar-like stars, which for a long time were not considered attractive astronomical targets. In the last decade, however, there has been a flourishing of studies, which also revealed some important relations between the presence of a planetary system and the properties of the host stars. One of the most relevant has been the work of Valenti & Fischer (2005), who found that extrasolar giant planets are more likely to form around metal-rich stars ([Fe/H]>0). More recently, Israelian et al. (2009) have found a negative correlation between the stellar lithium abundance and the existence of a planetary system, a correlation which is still under a vivid discussion. A detailed characterization of MS stars (atmospheric parameters and age)

is therefore fundamental in the understanding of planet formation and evolutionary status of the circumstellar disks of material which originate them.

In the case of intermediate- and late-type MS stars, chromospheric activity has been widely used as a clock[1], since the magnetic activity in the upper atmospheric layers is correlated with rotational period. Rotational periods are expected to decay as an effect of mass loss during the stellar lifetime. One of the most used indicators of chromospheric activity is the emission of the Ca H and K lines at 3969 and 3933 Å which is usually expressed as $R'_{HK} = L_{HK}/L_{bol}$, where L_{HK} is the luminosity within the emission lines and L_{bol} is the bolometric luminosity of the star. These transitions produce a strong photospheric absorption in solar-like stars but in an optically thin chromosphere, due to the temperature inversion, they generate emission lines (see Figure 1). The strength of this (sometimes very tiny) emission at the very center of a strong absorption feature has been correlated with age, by means of observations of stars in clusters of known age.

The recent R'_{HK}–age calibration of Mamajek & Hillenbrand (2008), which is shown in Figure 2, has been obtained from a collection of literature data for just about 200 stars of 13 open clusters (plus a small number of field stars of Valenti & Fischer (2005), whose age has been obtained by isochrone placement). They claim to have reached a relative precision of ∼60% for the age of solar analogs (in the age interval ∼0.6–4.5 Gyr).
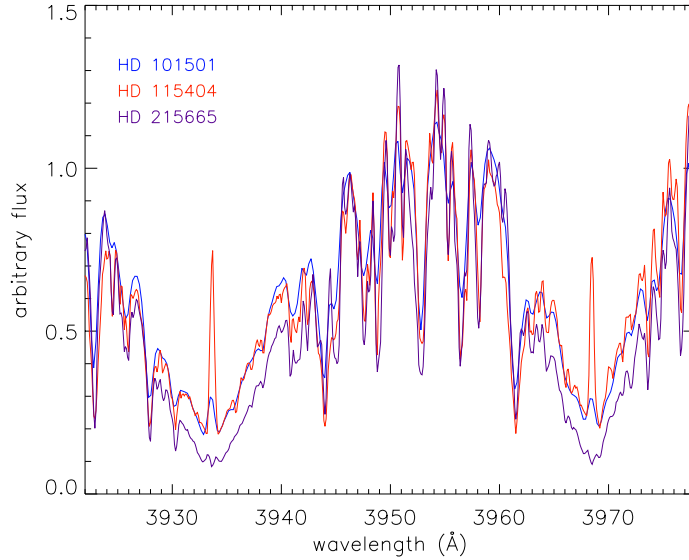
Fig. 1: The Ca H and K lines for three stars presenting different level of chromospheric activity. Spectral resolution is $R = 20,000$. [data from Montes et al. 1997]

---

[1] Other methods include nucleocosmochronometry, asteroseismology, kinematic analysis, lithium depletion, etc.
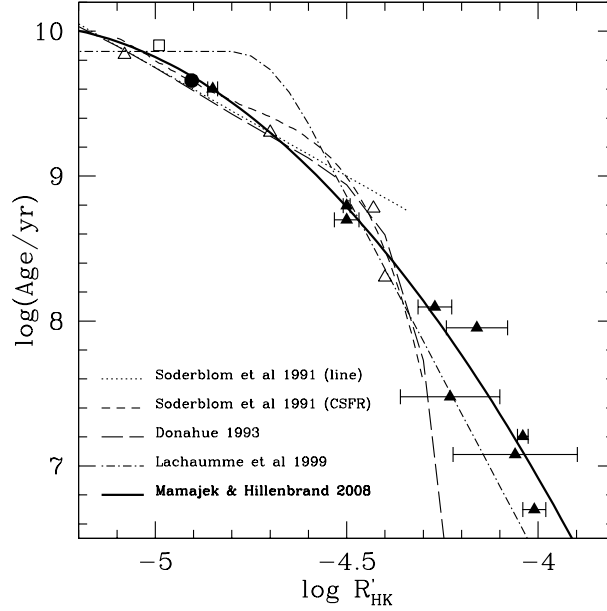
Fig. 2: The chromospheric activity–age calibration from Mamajek & Hillenbrand (2008), compared with previous calibration from different authors. The triangles show the mean $\log R'_{HK}$ values of star in cluster vs. cluster age; the square indicates the mean value for the sample of solar-type dwarfs from Valenti & Fischer (2005); the circle is the Sun.

2 The proposal

We propose to observe the Ca HK spectra of solar-type stars in a selected sample of 22 open clusters. These observations will considerably increase the number of cluster stars with a well measured R'_{HK}. This would allow to significantly decrease the uncertainty of the activity–age calibration, that we can be applied to field stars.

The sample of open clusters has been extracted from the WEBDA catalog[2] (Mermilliod J.-C. 2005), applying the following criteria:

a) $B \leq 18.5$ for a G2V type star;
b) a total number of stars with $B - V$ color typical of solar analogs (G0–G3 types) greater than 200;
c) a declination d$ec \geq -20$ deg.

The sample of the target open clusters is described in Table 1, where we report the name of the cluster along with the coordinates, the density of solar analogs, the diameter, the age, and the distance. It is worth noticing that our sample includes 6 clusters with age>1 Gyr. This age interval is critical, since the Mamajek & Hillenbrand (2008) calibration is based only on one bona-fide cluster in this range, since these objects are usually located at large distances from

---

[2] http://www.univie.ac.at/webda/

Table 1: The properties of the target open clusters.

Cluster name	RA	Dec	targets ($\#/arcmin^2$)	diam. (arcmin)	log Age	d (pc)
1 Stock 24	00 39 42	+61 57 00	108.5	5	8.08	2818
2 Berkeley 62	01 01 00	+63 57 00	80.2	5	7.18	1837
3 NGC 381	01 08 19	+61 35 00	102.5	6	8.51	1148
4 NGC 581	01 33 23	+60 39 00	295.3	5	7.34	2194
5 NGC 654	01 44 00	+61 53 06	86.5	5	7.15	2041
6 Berkeley 7	01 54 12	+62 22 00	57.5	4	6.60	2570
7 King 5	03 14 36	+52 43 00	68.7	5	9.00	1900
8 Berkeley 17	05 20 36	+30 36 00	115.4	7	10.08	2700
9 IC 2157	06 05 00	+24 00 00	103.9	5	7.80	2040
10 Saurer 1	07 18 18	+01 53 12	116.2	4	9.85	1970
11 Trumpler 32	18 17 30	-13 21 00	91.0	5	8.48	1720
12 NGC 6611	18 18 48	-13 48 24	75.9	6	6.88	1749
13 NGC 6631	18 27 11	-12 01 48	195.7	6	8.60	2600
14 Basel 1	18 48 12	-05 51 00	66.1	5	7.89	2178
15 NGC 6705	18 51 05	-06 16 12	63.7	13	8.30	1877
16 NGC 6819	19 41 18	+40 11 12	123.5	5	9.17	2360
17 NGC 6834	19 52 12	+29 24 30	72.2	5	7.88	2067
18 NGC 6996	20 56 30	+45 38 24	54.9	8	8.54	760
19 Berkeley 54	21 03 12	+40 28 00	198.5	4	9.60	2300
20 NGC 7235	22 12 25	+57 16 12	50.8	5	7.07	2823
21 King 11	23 47 48	+68 38 00	59.3	5	9.05	2892
22 NGC 7790	23 58 24	+61 12 30	133.3	5	7.75	2944

the Sun. The observations of a large number of stars in these evolved systems will greatly increase the precision of age determination for older stars.

As a first step, we plan to homogeneously derive the age of the clusters by using the latest Padova stellar tracks (Bressan et al., in preparation) to perform the isochrone fitting of the clusters' CMDs. The Padova group has recently revised their stellar evolution code, by including up-do-date physical ingredients (e.g., opacities, equation of state, nuclear reaction rates, chemistry, microscopic and turbulent diffusion, neutrino energy loss), and they have computed a new library of evolutionary tracks in a large range of age and metallicity ($0.15 M_\odot < M < 120 M_\odot$ y $0.0001 < Z < 0.05$). An extremely important property of these tracks is that they adopted the solar abundances from Ludwig et al. (2010), which has been obtained from 3D modelling of solar atmosphere and result in a total metallicity of $Z_\odot = 0.0153$[3]. Since for MS stars is the chemical composition (and not age) that defines their location on the CMD, the use of a new set of isochrones, based on different reference solar abundances, will give rise to a modified chronology, which will affect the stellar activity vs. age calibration.

[3] The Ludwig et al. values $Z_\odot = 0.0153$ is intermediate between the one proposed by Grevesse & Sauval (1998) ($Z = 0.0171$) and the one obtained by Asplund et al. (2005) ($Z = 0.0122$). However, the value of $Z = 0.0171$ is not compatible with the most recent observations, while the Asplund solar metallicity is in conflict with heliosesismological results.

3 The observations

Hectochelle will be used with the Ca41 filter, at a spectral resolution $R \sim 32000$, which is very suitable for detailed observations of emission at the core of the Ca HK lines (Fig. 1). With four hour exposure time observations, we should reach a SNR>10 for the Ca HK emission line even for the faintest stars of our sample and weak chromospheric activity.

The observation of the full sample of 22 clusters should use therefore about 100 hours (plus overheads) of telescope time.

4 Stellar atmospheric parameters

The spectra collected by the Hectochelle, in addition to the Ca HK chromospheric emission, will contain a wealth of information that can be exploited for determining the atmospheric parameters of all the observed stellar targets. The density of absorption lines in late-type stars is maximum in the blue interval and the $R \sim 32,000$ spectral resolving power, even if it is not enough to perfectly separate all individual lines, will certainly allow to define a set of line indices, that measure both the equivalent widths (or suitable Lick-like indices) and line flux ratios (e.g., Rose 1994; Liu et al. 2008), which have proved to be very sensitive to the main atmospheric parameters: effective temperature, surface gravity, and overall metallicity. The observed indices will be matched with those computed from a new library of suitable theoretical stellar spectra (Bertone et al., in preparation), which are being computed using the same solar partition of Ludwig et al. (2010) used to compute the new Padova evolutionary tracks. Before this comparison, however, the theoretical indices will be calibrated against the observations, using a suitable sample of well known reference stars.

References

Asplund, M., Grevesse, N., & Sauval, A. J. 2005, Cosmic Abundances as Records of Stellar Evolution and Nucleosynthesis, 336, 25

Grevesse, N., & Sauval, A. J. 1998, Space Sci. Rev., 85, 161

Liu, G. Q., Deng, L., Chávez, M., et al. 2008, MNRAS, 390, 665

Ludwig, H.-G., Caffau, E., Steffen, M., et al. 2010, IAU Symposium, 265, 201

Mamajek, E. E., & Hillenbrand, L. A. 2008, ApJ, 687, 1264

Mermilliod, J.-C. 1995, Information and On-Line Data in Astronomy, 203, 127

Montes, D., Martin, E. L., Fernandez-Figueroa, M. J., Cornide, M., & de Castro, E. 1997, A&AS, 123, 473

Rose, J. A. 1994, AJ, 107, 206

Soderblom, D. R. 2010, ARA&A, 48, 581

Valenti, J. A., & Fischer, D. A. 2005, ApJS, 159, 141

Massive stars in nearby galaxies

LUIS J. CORRAL AND SILVANA G. NAVARRO

Instituto de Astronomía y Meteorología, Universidad de Guadalajara

Av. Vallarta 2602, Col. Arcos Vallarta Sur, C.P. 44130, Guadalajara, Jalisco, México

INSTRUMENT: BINOSPEC

1 Scientific context

Massive stars are the origin of several highly energetic phenomena. Born with masses exceeding eight times the solar mass, they are one of the main sources of the chemical and dynamic evolution of galaxies. Its evolution is very fast, and during their life time releases large amounts of nuclear-processed material through fast and dense stellar winds. As a very powerful source of high-energy photons, they are responsible of the heating and ionization of interstellar material. They will die as supernovae at the end of his life, injecting more chemical enriched material and turbulent energy to the interstellar medium. The remanets are neutron stars or black holes and some of them can produce Gamma Ray Bursts.

Massive stars are also very luminous and can be studied individually on nearby galaxies, they can used as standard candles to find their distance. The evolutionary process vary with the physical properties of the stars, like the initial mass, metallicity and rotation velocity. Metallicity depend on the galaxy that hosts the stars and in some of the nearby galaxies the properties that we found are close to those in the early Universe. This give the chance to understand the process that took place when the universe was young and the first stars was formed. When we observe distant galaxies we have the contributions of many type of stars integrated in the radiation, therefore is necesary to study massive stars with different evolutionary stages in several nearby galaxies that cover a variety of these parameters.

One of the stages of the evolution of massive stars are known as Luminous Blue Variables (LBV). These are a group of irregular variables characterized by their intrinsic high luminosites, blue colors, their photometric behavior and their related spectroscopic changes. Members of this group have been identified not only in the Milky Way, but in nearby galaxies as well. LBV is a term coined by Conti (1984) that covers member of the S Dor variable, the Hubble-Sandage variable and the P Cygni variable classes. Reviews of LBV can be found in Humphreys & Davidson (1994), and in Bohannan (1997). In M 33 there are at least 6 known LBV. Four of them were identified first by their variability: Var B, Var C, Var 2 (Hubble & Sandage 1953) and Var 83 (van den Bergh et al. 1975). Recently three more LBV have been identified in M33: B 324, UIT 003 and B 416. (Monteverde et al. 1996, Massey et al. 1996 and Shemmer et al. 2000)
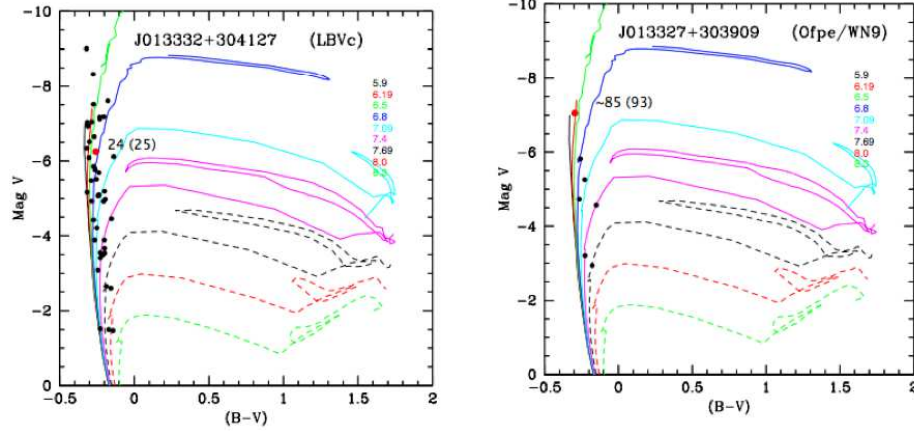
Fig. 1: HR diagrams of two clusters with a LBVc member (in red) of M 33. The tracks are isocrons calculated by Lejeune & Schaerer (2001) and the masses are the initial mass of the objects.

Some stars with the same, or at least related, spectroscopic characteristics of LBV, but without any reported variation in historical times, are known as LBV-candidates (LBVc). There are at least 15 stars classified as such in the literature that belong to M33 (see Massey et al. 1996 and Corral 1996). The importance of the number of LBV in a particular galaxy, is that this number is directly related with the lifetime of this evolutionary stage. Is during this phase that the strongest mass loss rates are found in the evolutionary track of massive stars (Humphreys & Davidson 1994), and is believed that the LBV phase is previous to the WR phase in some of the most massive stars. The masses of WR found in binaries are in the order of 5 to 10 $M_\odot$, but objects in the previous phases are in the order of 20 $M_\odot$ or more. Is expected that during the LBV phase at least 5 (or even 10) $M_\odot$ are lost, making a great contribution to the input of momentum and chemical enrichment to the interstellar medium. We want to determine the mass and age of these objects learn if all the massive stars go through this stage or only the most massive ones.

2 Proposed methodology

A well known method of understanding the nature of evolved stars is to determine the turn-off luminosities on the HR diagrams of clusters containing such objects (Johnson & Sandage 1955; Schwarzschild 1958) and with evolutionary theory results determining the age of the cluster. This was first applied by Sandage (1953) to get the masses of RR Lyrae stars in the globular clusters M3 and M92 (Sandage 1956). In a previous work (Corral et al. in preparation) we found the HR diagrams of massive star clusters and associations with an LBV or LBVc members. Ussing evolutionary tracks calculated by Lejeune & Schaerer (2001) we found that photometrically they show a variety of masses (from 25 to > 100 $M_\odot$). We need to study the members of the cluster spectroscopically to better determine their paremeters

(mass, log g, metallicity, mass loss rate and rotational velocity) and discard those objects that are binaries (or multiples) in order to get a better understanding of the evolution. These studies can be done with BINOSPEC. Their multi object spectroscopic capability, the wide field of view (16 x 15) and high throughput (30% @ 5000 Å) make it a very usefull instrument to this kind of studies. We propose to observe a good sample of the memeber of the cluster and found their parameters comparing the sepectrum with models calculated with the code CMFGEN.

References

Bohannan, B., in Luminous Blue Variables: Massive Stars in Transition, 1997, ASP Conf. Series, 120, Nota, A., Lamers, H.J.G.L.M. eds.

Conti, P.S., in Observational tests of the stellar evolution theory, 1984, IAU symp. 105, ed. Maeder & Renzini (Kluwer, Dordrecht), p. 233

Corral, L.J., 1996, AJ, 112, 1450

Herrero, A., Lennon, D.J., Vilchez, J.M., Kudritzki, R.P.. Humphreys, R.H., 1994, A&A, 287, 885

Hubble, E. & Sandage, A., 1953, ApJ, 118, 353

Humphreys, R. & Davidson. K., PASP, 1994, 106, 1025

Johnson, H. L., & Sandage, A. R. 1955, ApJ, 121, 616

Lejeune J. & Schaerer D. 2001, A&A, 366, 538

Massey, P., Bianchi, L., Hutchings, J.B., Stecher, T.P., 1996, ApJ, 469, 629

Monteverde, M., Herrero, A., Lennon, D., Kudricki, R., 1996,A&A, 312, 24

Sandage, A. 1953, Mem. Soc. Roy. Sci. Liege, 14, Ser. 4, 254

Shemmer, O, Leibowitz, E. M., Szkody, P., 2000, MNRAS, 311, 698

van den Bergh, S., Herbst, E., Kowal, Ch., 1975, ApJS, 29, 303

The impact of massive outflows in Galactic Star Formation

ARTURO GOMEZ-RUIZ

Instituto Nacional de Astrofísica, Óptica y Electrónica
Luis Enrique Erro 1, Tonantzintla, Puebla, México

POTENTIAL INSTRUMENTATION: MMIRS + LMT

1 Introduction

Understanding the formation of High-Mass stars is one of the main problems of the modern astrophysics. In recent years, unbiased surveys in the Mid-IR and Sub-mm have given us new samples of candidates of High-Mass Protostars in the earliest phase of formation. Systematic studies trying to characterize such objects are underway. An example of these is the GLIMPSE (Galactic Legacy Infrared Mid-Plane Survey Extraordinaire) survey in the Mid-Infrared (Mid-IR), from which different star-formation phenomena have been revealed, from Ultra Compact HII regions to bipolar outflows.

A new catalog of massive outflows has been published by Cyganowski et al. (2008), based on the GLIMPSE survey with the IRAC camera. The finding method consisted in displaying three color images (3.6, 4.5 and 8.0 μm) of the GLIMPSE survey area and look for Green Extended Objects (EGOs, with the 4.5 μm band coded as green). Observationally, the excess in the 4.5 μm band is interpreted as a shock tracer based on comparisons with Near-IR H_2 narrow-band images and the presence of the H_2 lines and CO bandheads in this band (Davis et al. 2007). The gas temperatures implicated are > 1000 K, and therefore tracing very energetic outflows (Ybarra & Landa, 2009). This extended emission is interesting as a new diagnostic for Massive Protostars, in particular the outflows related with them. This catalog compile around 300 extended 4.5 μm sources, most of them new massive outflow candidates, not studied before in any other outflow tracer. Recently, Chen et al. (2013) added about one hundred more newly identified EGOs from the GLIMPSE II survey.

Near- and mid-IR observations of massive outflows with SPMT

The relevance of such EGOs is that those sources with an excess in the 4.5 micron band could be related with the earliest phases of massive star formation, as well as revealing
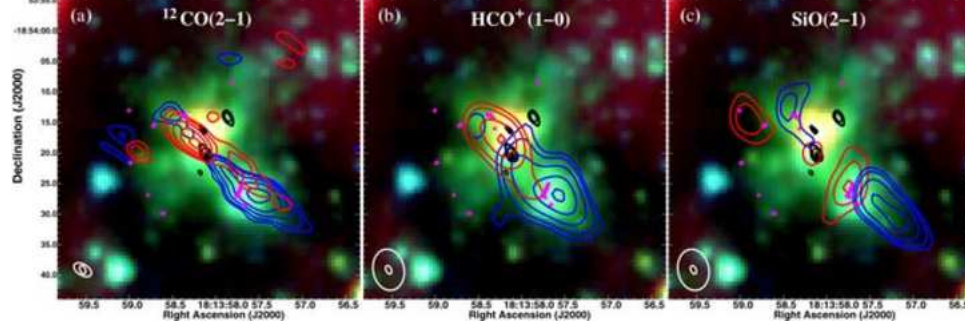
Fig. 1: The three color image from the GLIMPSE/IRAC survey showing an Extended Green Object, while the contours show molecular line observations demonstrating that EGOs are tracing molecular outflows (from Cyganowski et al 2011a). An image similar to these could be provided by data from the SPMT and the LMT (at infrared and millimeter wavelengths, respectively).

very energetic outflows which could have a very important impact in the ISM as a whole: shock-induced chemistry and shocks as a feedback process. Follow up observations have started trying to characterize EGOs by using several star formation tracers. In particular, Cyganowski et al. (2009, 2011a,b) have presented interferometric observations of centimeter continuum emission, CH_3OH masers, CO, SiO, and HCO^+ transitions in a sub-sample of about 20 EGOs, tracing ionized regions and molecular outflows, suggesting that EGOs are related with massive outflows (see Fig. 1). In the infrared, the most complete study comes from Lee et al. (2013), whose narrow band H_2 and continuum near-infrared observations in about 90 EGOs showed that only half of them were related with H_2 outflows (considering the H_2 outflows incompleteness), while the rest comes from scattered continuum from the embedded young stellar object. The discrepancy between the radio/mm and NIR observations may come from the different optical deeps each tracer is sensitive to and/or the low statistics in the radio/mm data. These results therefore call for further investigations in the radio/mm, NIR, and Mid-IR wavelengths, in the latter case with direct spectroscopy of the 4.5μm band.

NIR observations with a 6-m class telescope will be key to complete the H_2 survey towards this sample of massive outflows candidates, for example with an instrument like the MMIRS. With its sensitivity and angular resolution, detailed analysis of the emission structures can be made, and faster than with previous observations. These observations will complement an observing campaign our group at INAOE will undertake with the Large Millimeter Telescope in molecular lines. The synergy between these two facilities will provide an advantage in the data analysis. However, what would be really new is to enable the 6-m SPMT with mid-IR spectrographs, in order to provide direct spectroscopy in the 4.5μm band, which has been barely tried until now, at least in these objects.

In general, the 6-m SPMT will be a very important facility which can work very well in synergy with the LMT, since in the particular case of outflows studies infrared data is key for the development of the next generation models that try to explain the mechanisms behind the outflow phenomenon in star formation. Therefore, the SPMT together with the LMT will provide an important advantage to Mexican community working in this field.

References

Chen et al. 2008, MNRAS, 396, 1603
Chen et al. 2013, ApJS, 206, 9
Cyganowski et al. 2011a, ApJ, 729, 124
Cyganowski et al. 2011b, ApJ, 743, 56
Cyganowski et al. 2008, ApJ, 136, 2391
Cyganowski et al. 2009, ApJ, 702, 1615
Davis et al. 2007, MNRAS, 374, 29
Ybarra & Lada, 2009, ApJ, 695, L120

Symbiotic systems and planetary nebulae: determination of physical parameters

SILVANA G. NAVARRO JIMÉNEZ

Instituto de Astronomía y Meteorología, Universidad de Guadalajara
Av. Vallarta 2602, Col. Arcos Vallarta Sur, C.P. 44130, Guadalajara, Jalisco, México

INSTRUMENT: BINOSPEC

1 Scientific Aim

Symbiotic systems are binary systems that undergone mass transfer episodes in their evolution history, producing in some cases accretion disks, and in many of these objects are observed collimated mass ejection. Planetary nebulae are the result of the evolution of low and medium mass stars, when the evolved star are part of a binary system, it could transfer mass to the companion when it transform into an AGB or Mira variable. The physical process in both type of objects are very similar and many authors coincide in the probable evolutionary relation between them. The binary periods determined for some of these objects are very different: from few months or years for PNe to more than ten years for SS.

In the other hand, many PNe shows multiple rings and structures that may be the result of multiple mass loss episodes and, in many cases the interaction between material from them produce shocks. The analysis of the emission lines observed in these objects: $\lambda\lambda$ 4363 and 5007, from [OIII], Hβ, Hα and $\lambda\lambda$ 6548 and 6583 from [NII] and their quotients may give us an idea of the process producing these lines (photoionization or shocks) troughout the construction of diagnostic diagrams. The weak emission from the rings and halos in PNe demand the use of a large telescope (in the range of 6 to 10 m) with image and spectral capabilities, for this reason BINOSPEC will be the ideal instrument.

The recent results of the IPHAS project (Viironen et al. 2009, Sabin et al., 2014.) produce a good number of candidates to PNe many of them with weak emission lines. The possibility to use a 6.5m telescope let us to obtained reliable spectroscopy that could confirm such classification and permit us to obtain the physical parameters of each nebula.

2 Methodology

The analysis of the emission lines observed in these type of objects, and the construction of the appropriate diagnostic diagrams can separate the Symbiotic systems from the PNe: 5007/4363 vs 4363/4340 (Gutierrez-Moreno et al. 1995) (Figure 1) Another diagrams can give evidence for shocks in this objects.

The determination of electron density (ne) and temperature (Te) can be made from the $\lambda\lambda$ 4363 and 5007, [OIII] lines, Hβ, Hα, $\lambda\lambda$ 6548 and 6583 [NII] lines, and $\lambda\lambda$ 6717 and 6730 [SII] emission lines, using the equations from Osterbrock & Ferland, 2006.

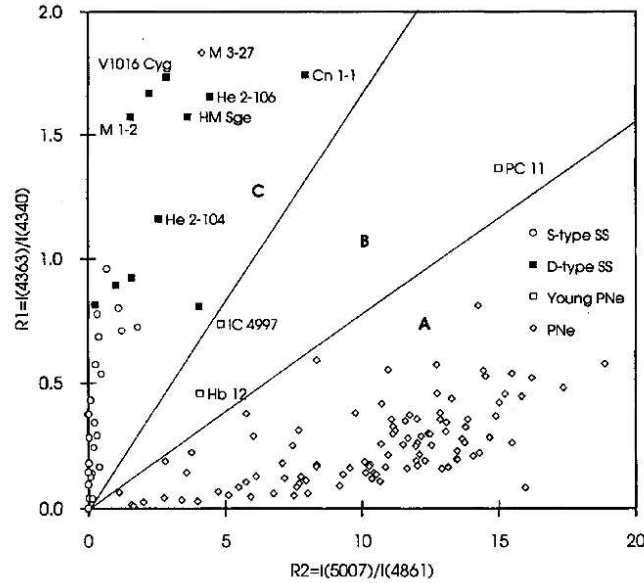Fig. 1: Diagram from Gutierrez-Moreno et al. Where the clear separation of PNe and simbiotics is shown.

References

Gutierrez-Moreno A., Moreno, H. & Cortés. 1995. PASP, 107, 462.
Osterbrock, D.E. & Ferland G. J., 2006. Astrophysics of gaseous nebulae and active galactic nuclei
Sabin, L.; Parker, Q.A.; Corradi, R.L.M.; et al. 2014. MNRAS 443, 3388
Viironen, K.; Greimel, R.; Corradi, R.L.M.; et al. 2009. A&A, 504, 291

Molecular hydrogen of small scale structures in planetary nebulae

GERARDO RAMOS LARIOS, LAURENCE SABIN AND MARTIN A. GUERRERO

Instituto de Astronomía y Meteorología, Universidad de Guadalajara
Av. Vallarta 2602, Col. Arcos Vallarta Sur, C.P. 44130, Guadalajara, Jalisco, México

POTENTIAL INSTRUMENTATION: MMIRS + MEGACAM

1 Introduction

One of the most attractive and interesting aspect of the study of Planetary Nebulae (PNe), which are the product of the evolution of low and intermediate mass stars (0.8M 8M$_\odot$), resides in their outstanding morphologies. The observed shapes originate from the successive mass loss events occurring during the PN formation process (coupled with other physical mechanisms), which ultimately led to the formation of an extensive ionized nebula (Kwok 2000). The latter will then slowly dissipate into the interstellar medium (ISM).

The morphological analysis (of macro and micro structures) of these nebulae has been at the centre of various investigations related to the creation of morphological catalogues (e.g. Sahai et al. 2011) underlying the wide variety of shapes and therefore the occurrence and implication of (a) distinctive shaping mechanism(s); the determination of the kinematics of the ionised ejecta (e.g. López et al.2012) or the analysis of the faint ejecta (halos) from the Asymptotic Giant Branch phase which are sometime still observable around PNe (e.g. Ramos Larios & Phillips 2009, Corradi et al. 2003).

While most of these morphological investigations were generally made using deep optical images focusing on emission lines such as Hα, [N II] 6584 and [O III] 5007, it has been noted that PNe can also be well imaged using molecular lines in the near infrared such as H$_2$. This weak emission line has the advantage not only to indicate the bipolar nature of PNe (Kastner et al. 1996) by underlying the contours of the dark lane or the disk/torus where H$_2$ is not dissociated; but also to delineate the transition zone between the ionised and molecular regions in the nebulae. In this framework several investigations have been realised and we can cite as an example the works by Cox et al. 2001, Volk et al. 2004, Matsuura et al. 2009 and Marquez Lugo et al. 2013, Guerrero et al. 2013 [and references therein], which mainly targeted large and/or bright PNe.

The aim of this proposal is to search for H$_2$ (1-0) S(1), H$_2$ (2-1) (S1) and Brγ line emission in the near IR K band of small scale low ionisation structures of PNe in order to assess the origin of the mid IR emission and to derive line ratios in the H$_2$ lines to study the excitation
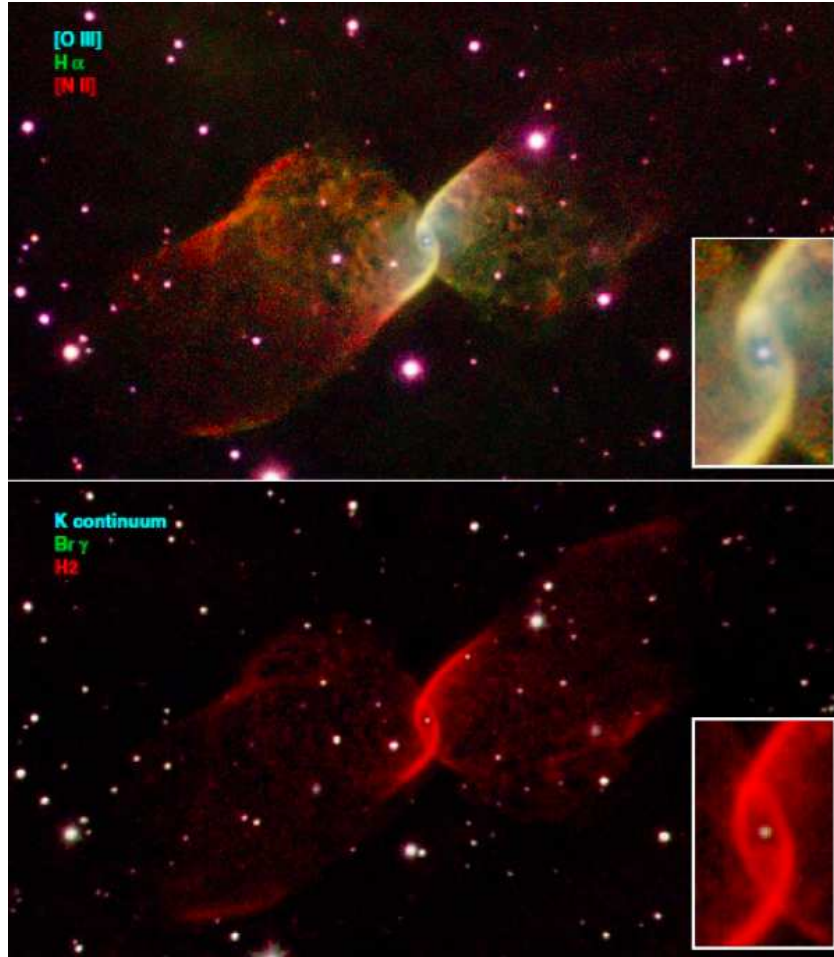
Fig. 1: NOT telescope color composite optical (top) and WHT telescope near IR (bottom), narrow band pictures of PN Kn 26. The narrow band filters and colors assigned to each picture are labeled on them. The FoV is $150'' \times 85''$. In both pictures north is up, east to the left (Guerrero et al. 2013).

mechanisms: ionized gas would imply Brγ emission, molecular material would result in the detection of H$_2$ emission, and dust would result in neither detection of Brγ nor H$_2$ emission.

With these observations we expect to achieve several goals: corroborate for the first time the presence (or absence) of molecular hydrogen in small or distant PNe and then identify the nature of the emission at distinctive locations, compare the optical and Near IR morphologies in the case of a positive detection as well as evaluate the evolution of H$_2$ for PNe presenting similar morphologies but different evolutionary stage.

References

Corradi R. L. M., Schönberner D., Steffen M., Perinotto M., 2003, MNRAS, 340, 417

Cox, P., Lucas, R. Huggins, P., Maillard, J.P.
Post-AGB Objects as a Phase of Stellar Evolution, Proceedings of the Torun Workshop held July 5-7, 2000. Edited by R. Szczerba and S. K. Górny. Astrophysics and Space Science Library Vol. 265, ISBN 07923-71453. Publisher: Kluwer Academic Publishers, Boston/Dordrecht/London, 2001.

Guerrero, M. A., Miranda, L. F., Ramos-Larios, G., Vázquez, R., A&A 2013, 551, A53

Kastner, J;., Weintraub, D., Gatley, I., Merrill, K. M., Probst, R., ApJ, 1996, v.462, p.777

Kwok, S. Asymmetrical Planetary Nebulae II: From Origins to Microstructures, ASP Conference Series, Vol. 199. Edited by J. H. Kastner, N. Soker, and S. Rappaport. ISBN: 1-58381-026-9, 2000, p. 9

López, J. A., Richer, M. G., García-Díaz, M. T., Clark, D. M., Meaburn, J., Riesgo, H., Steffen, W., Lloyd, M.
Revista Mexicana de Astronomía y Astrofísica, 2012, Vol. 48, pp. 3-7

Marquez-Lugo, R.A., Ramos-Larios, G., Guerrero, M.A., Vázquez, R. MNRAS 2013, 429, 973

Matsuura, M., Speck, A. K., McHunu, B. M., Tanaka, I., Wright, N. J., Smith, M. D., Zijlstra, A. A., Viti, S., Wesson, R., ApJ, 2009, Volume 700, Issue 2, pp. 1067-1077

Ramos-Larios, G., Phillips, J.P., MNRAS, 2009, 400, 575

Sahai, R., Morris, M., Villar, G., AJ, 2011, 141, 134 (31pp)

Volk, K., Hrivnak, B., Kwok, S., ApJ 2004, Volume 616, Issue 2, pp. 1181-1187

Observing Near Earth Objects using the 6.5m TSPM

Mauricio Reyes Ruíz, Mónica W. Blanco Cárdenas, Roberto Vázquez Meza, Carmen Ayala, Manuel Núñez

Instituto de Astronomía, Ensenada, Universidad Nacional Autónoma de México
Km. 103 Carretera Tijuana-Ensenada, C.P. 22860, Ensenada, Baja California, México

Potential instrumentation: Megacam + MMIRS

1 Introduction

The Near Earth Objects (NEOs) are defined as those minor bodies of the Solar System with orbits close to our Planet (0.983 to 1.3 AU) and its population is constituted by different type of objects: meteoroids, asteroids, comets, interstellar dust, and interplanetary dust particles (Binzel et al. 2002). The study of NEOs has relevant implications for the international astronomical community. First, some of these objects preserve properties of the primordial conditions of the Solar System, as has been revealed by in situ measurements and astronomical observations. Moreover, the exploration of space mining is opening a new window in this research area, through the resource exploitation of nearby asteroids. On the other hand, as they reach and/or cross the orbit of the Earth, the possibility of impact must be considered as we trace contingency plans and make a detailed evaluation of the damages that these events may produce.

It has been estimated that nearly 50 to 150 tons of dust and small objects break through the atmosphere each day without any catastrophic consequences, however, those big enough to produce craters have impacted the Earth before and they are associated with massive extinctions (e.g. the 10 Km Chicxulub crater in Yucatán, Mexico). Furthermore, even when small objects of few tens of meters go through the atmosphere and disintegrate without a collision with the ground, considerably local damage may be provoked (e.g. Tunguska and Chelyabinks on 1908 and 2013, respectively).

The NEOs are classified by its chemical composition, like the asteroids, and, due to these chemical properties, they can be highly reflective or obscured at optical wavelengths and, above all, knowing its chemical composition is critical to understand the damages generated in case of collision with the Earth. Nowadays, more than 11,000 NEOs have been discovered thanks to the effort of several missions devoted to this task. However, those with diameters below 140 m and likely a high fraction of the reddest (low albedo objects and, thus, strong infrared emitters) remain unknown. Therefore, to properly characterize these objects several studies may be performed.

In this context, taking advantage of the construction of the 6.5 m telescope in San Pedro Mártir (hereafter referred as TSPM) we have explored the possibilities of using this powerful telescope to study NEOs. In the following lines, we describe three projects to detect and characterize NEOs using the Magellan/MMT/TSPM instruments approved for the collaboration.

2 Deep NEOs survey

Due to its 6.5 m aperture, the TSPM operating with the wide field camera MEGACAM (field of view $24'x24'$) offers a valuable opportunity to accomplish a deep survey of NEOs focused in the study of the statistical properties of the orbital distribution of these objects, as well as their sizes. One of the most important parameters of the NEOs is the absolute magnitude H, which is related to the size of the object and its albedo. The usage of MEGACAM/TSPM will allow to seek and observe smaller NEOs, down to few tens of meters in size, due to its higher sensitivity, compared with the rest of the surveys devoted to this effort. In comparison with other surveys, such Catalina sky Survey (CSS), Pan-STARRS, and the forthcoming Large Synoptic Survey Telescope (LSST), the MECAM/TSPM deep survey will focus in a limited field or in a group of fields (a.k.a. pencil-beam survey), accordingly to the observing time granted to this project. Further, the sensitivity will be greater than the sensitivity achieved by Pan-STARRS and by the pencil-beam survey DECam (Dark Energy Camera NEO Search Program, CTIO). The main goals of this survey are: 1) To detect less brighter NEOs, because of their small size, their low albedo or because they are away on its orbit and 2) To determine the orbital distribution by means of statistics and their sizes with the highest sensitivity possible. Both quantities are fundamental to know the impact probability and the risks that the NEOs population may imply. Finally, we have investigated possible observation strategies leading us to an estimation of several hundreds of NEOs discovered by this deep survey.

3 Rapid-response taxonomy

As was mentioned before, knowing the chemical composition of NEOs is vital to prevent and to trace contingency plans in case of impact. The surveys dedicated to detect NEOs have a magnitude limit of V=20, the objects bright around this magnitude, typically during several weeks, until they diminish its bright just before they are not observable at all. Thus, the only way to characterize these objects is to observe them immediately after their discovery. One of the most used methods to inspect the composition of NEOs is to perform photometry in different bands to infer some properties of the reflectance spectrum of these objects. The 8-color classification system proposed by Tholen (1984) is one of the most used and provides a preliminary and useful overview of the composition of these objects. The instrument MMIRS mounted in the TSPM will allow to perform these photometric observations in the Y, J, H, and K near infrared bands for the more obscured NEOs, since they are strong infrared emitters, helping us to constrain their albedo, a critical parameter to estimate the size of these objects. A significant improvement to the MMIRS observations devoted to this project would be to acquire a z filter, without substantial expenses and easy to implement as well. Finally,

it is worth to mention that the MMIRS/TSPM project will complement the LSST project, providing the missing infrared information of the LSST.

4 Characterization of NEOs

To precisely determine the mineralogy of NEOs, optical and infrared spectroscopic observations are required. Considering the 1st generation of instruments of the TSPM, the usage of MMIRS on its long-slit observing mode will offer a valuable opportunity to achieve a fine characterization of most obscured NEOs. Beside a red slope on their reflectance spectrum, carbonaceous and metallic NEOs show considerable differences at near infrared wavelengths. For example, the presence of absorptions at 1 and 2 microns indicate a silicate mineralogy, and their relative abundances and centers tells us what kind of silicate (olivines and piroxenes) dominates the composition of the NEO observed. Furthermore, NEOs with sizes down to 500 m have no spectral information at all. The NEOs characterization project using MMIRS/TSPM will open a new and excellent opportunity to contribute to the international efforts to the knowledge of the properties of the NEO population. Finally, the execution of all these projects are planned in the queue observation mode proposed for the operation of the TSPM.

References

Binzel et al. 2002
Tholen 1984

High resolution spectroscopy and the abundance discrepancy problem in ionized plasmas

MICHAEL RICHER ET AL.

Instituto de Astronomía, Ensenada, Universidad Nacional Autónoma de México
Km. 103 Carretera Tijuana-Ensenada, C.P. 22860, Ensenada, Baja California, México

POTENTIAL INSTRUMENTATION: MAESTRO

1 Scientific context

Ionized gas is used to infer chemical abundances throughout the universe. Usually, these abundances are derived from observations of strong, collisionally-excited emission lines. However, in the local universe, it has long been known that the abundances derived from these lines differ from those derived from recombination lines, at least for the common ions C^{++}, N^{++}, O^{++}, and Ne^{++} (Wyse 1942; Peimbert & Peimbert 2006; Liu 2010). This problem is known as the abundance discrepancy problem. Typically, in H II regions, the abundances inferred from recombination lines are about a factor of two larger than those inferred from collisionally-excited lines. In planetary nebulae, the same situation holds for about 80% of the objects studied thus far, but the remaining objects have larger discrepancies, exceeding a factor of five (Liu 2010). There is presently no completely satisfactory explanation for this abundance discrepancy. Although it is impossible to study this problem in the more distant universe in the spectra of active galaxies, since their internal kinematics smear the spectra too much to distinguish the individual recombination lines, there is no reason to expect that it does not exist, leading Ferland (2003) to classify the issue among the big, unsolved problems facing nebular astrophysics and our understanding of the chemical abundances in ionized plasmas throughout the universe. This issue is not trivial, since these elements are among the most common in the universe, but are created in stars. The implications therefore extend beyond nebular astrophysics to the understanding of both stellar evolution (and perhaps structure) and the cycling and accumulation of matter within the galaxies they inhabit.

Thus far, most studies of the abundance discrepancy problem have used low-resolution spectroscopy. While this has permitted the problem to be characterized in many objects, it has the consequence of integrating the physical conditions (and the physics) along the line of sight through the objects studied. High-resolution spectroscopy can and should be pursued vigorously, as it can take advantage of the internal kinematics to resolve the H II regions and planetary nebulae of interest along the line of sight and also allow the study of the physical conditions locally, resolved along the line of sight.

Recently, we used high-resolution spectroscopy obtained with the UVES spectrograph at the VLT to compare the kinematics of recombination and collisionally-excited emission lines through NGC 7009 (Richer et al. 2013), finding an additional kinematic component emitting in recombination lines, but with no counterpart in collisionally-excited lines. In other recent studies (Peimbert & Peimbert 2013, Peimbert et al. 2014), we have used low-resolution spectroscopy to compare the temperatures, densities, and pressures inferred from recombination and collisionally-excited lines in H II regions and planetary nebulae, including NGC 7009, finding rather similar physical conditions for both types of lines. Since the first study is nearly unique, its results cannot be generalized yet and so must be repeated in more objects to understand whether its result is typical. The second type of study has already been applied to a number of objects, so its results are clearly more general, but it would be useful to study some of the same objects at high spectral resolution to determine whether the results hold both locally and globally (resolved and integrated along the line of sight, respectively). Both types of studies would provide crucial information to better understand the conditions under which the recombination and collisionally-excited emission lines are emitted in ionized plasmas, both in the local and distant universe.

For both types of studies, which provide crucial information to understand the origin of the abundance discrepancy problem, access to a world-class, high-resolution spectrograph is necessary. The Maestro spectrograph, used with the atmospheric dispersion corrector at the f/5 focus of the MMT, should be a capable of undertaking the required studies. The spectrograph s design optimizes its performance in the UV and blue parts of the spectrum, coinciding with the wavelength range that includes the majority of the emission lines of interest.

References

Ferland, G. J. 2003, ARA&A, 41, 517

Liu, X.-W. 2010, in NewVision 400: Engaging Big Questions in Astronomy and Cosmology Four Hundred Years after the Invention of the Telescope, ed. D. G. York, O. Gingerich, S.-N. Zhang & C. L. Harper, Jr. (arXiv:1001.3715v2)

Peimbert, M., & Peimbert, A. 2006, in IAU Symp. 234, Planetary Nebulae in our Galaxy and Beyond, ed. M. J. Barlow & R. H. Méndez (Cambridge: Cambridge Univ. Press), 227

Peimbert, A., & Peimbert, M. 2013, ApJ, 778, 89

Peimbert, A., Peimbert, M., Delgado-Inglada, G., García-Rojas, J., & Peña, M. 2014, RMxAA, 50, 329

Richer, M. G., Georgiev, L., Arrieta, A., & Torres Peimbert, S. 2013, ApJ, 773, 133

Wyse, A. B. 1942, ApJ, 95, 356

Young star clusters and the structure of molecular clouds with the TSPM

Carlos Román Zúñiga

Instituto de Astronomía, Ensenada, Universidad Nacional Autónoma de México
Km. 103 Carretera Tijuana-Ensenada, C.P. 22860, Ensenada, Baja California, México

Potential instrumentation: Hectochelle, Megacam, MMIRS

1 Young Star Clusters

A majority (70-90%) of the stars in our Galaxy –and most likely in other galaxies too– form in relatively numerous groups (typically, hundreds to thousands of members). These stellar nurseries are known as embedded clusters. They are detected though surveys of Giant Molecular Cloud complexes with active star formation, where they are usually still forming a fraction of their members while still being surrounded by the remnant of the parental gas clumps from which they formed. Embedded star clusters are difficult to observe in optical wavelengths due to the copious amount of dust usually present in the cluster envelopes, but they are usually very bright –prominent, in fact– at infrared wavelengths (Lada & Lada, 2003).

To understand the processes of formation and early evolution of these young stellar systems is a problem that sits at the very backbone of modern astrophysics, relating two fundamental, unsolved puzzles: the process of star formation, and the process by which galaxies assemble from the stars formed in the clusters. To understand embedded star clusters takes us to understand basic questionings like: why are stars preferentially formed in numerous groups and not in small or isolated systems?, how important is the influence of local environment to define the properties of the clusters they form (Román-Zúñiga 2014)?, how is that star clusters have so similar Initial Mass Function (IMF) despite forming in completely independent regions (Bastian et al 2010)?, is the IMF assembled since the fragmentation of the molecular cloud itself (Alves et al 2007)? The answers we can give to these questions is what eventually will lead us to tackle more complex problems, like what were the process by which globular clusters or dwarf galaxies were assembled (Kissler-Patig et al 2006)?, how massive clusters can be formed in very small galaxies with relatively little gas (de Grijs 2013)?

To date, embedded clusters in relatively nearby active star forming complexes, like Orion, Perseus or Taurus, have been studied with meticulous detail. In those nearby (d < 500 pc) complexes we can resolve binary or multiple systems, or detect very low mass sources, even with relatively small telescope apertures. For instance, class 2-4m equipped with sensitive infrared cameras are enough to sample the mass spectrum of a nearby embedded cluster down

to the brown dwarf regime $(0.005 - 0.02 \ M_\odot)$. The problem is that, at smaller distances, the area of a cluster with 103-104 members can easily span from a few to a few tens of square degrees. Thus, global studies in complexes like Orion or Perseus, aimed to study environmental process or the interaction between clusters, require of capital observational effort. For that reason, global studies of molecular complexes that consider entire "families" of clusters are better suited for more distant regions (e.g. the Rosette Molecular Cloud, W3; Román-Zúñiga et al. 2008, 2015). Class 4-6m or 6-8m telescopes are nowadays being used to augment the level of detail in complexes at distances of 1 to 2 kpc.

Surveys of numerous star cluster forming regions have been done from both earth and space-based facilities. However, most of these studies do not include high resolution spectroscopy data, capable of providing radial velocities to trace the internal kinematics of the clusters. Only a handful of studies have succeeded at this task so far (e.g. Fürész et al 2006,2008; Cotaar, 2015). These data are crucial to understand one essential aspect: how a few embedded clusters survive to become bound open clusters while the rest do not (the so called "infant mortality", Lada & Lada 2003). Two aspects of this problem are important: a) the removal of the gravitational potential formerly provided by the parental gas once it is removed, and b) the effect of tides both from the cloud and nearby clusters (the so called "cruel cradle" effect, Kruijssen) and from the gravitational potential of the Galaxy. Also, this could help to attack another poorly understood aspect: the evolution of star clusters -manifested as variations in their size, density and morphology- from sub-virial states.

UNAM is already actively participating in a systematic large scale study of nearby ($d <$ 500 pc) young star cluster kinematics in the "Young Clusters and Young stars" goal science group (Covey et al. 2013) of the APOGEE-2 survey of the fourth phase of the Sloan Digital Sky Survey (SDSSIV). However, this survey, performed with the Apache Point 2.5m telescope, is limited to the brightest population (H[1.6 μm] $<$ 12.5 mag) of the clusters. An instrument like Hectochelle, would allow, undoubtedly, to perform similar systematic studies of the velocity dispersion in young clusters both down to the low mass end in nearby clusters, or to extend the reach to more distant (d>1 kpc) regions. To date, studies like those of Fürész et al. (2006, 2008) show clearly the feasibility of such projects down to 1 kpc. In Fig. 1 we show an image of the W3 complex (Román-Zúñiga et al 2015), where we can see the spatial distribution of over a thousand young stars with ages between 1 and 3 Myr, identified and classified from multi-wavelength photometry catalogs (infrared plus X-rays). The approximate diameter of this region is 1 degree, ideal for Hectochelle (to measure radial velocities) or Hectospec (to classify spectral types and/or determine stellar masses). The difference respect to studies of nearby regions is that we would be able to study the interaction between different clusters and the relation to the molecular cloud as it is being evacuated from the complex.

Nowadays, Hectochelle is in doubt for being included in the package of f/5 instruments to be moved to the TSPM. One of the main reasons for this is the current status of the fiber positioning system and head, which is possibly reaching the end of its operating life. However, we would like to propose here a possible solution to the problem: the idea is that, based on the experience we are acquiring from APOGEE-2, we could consider to design and construct a replacement, simpler system of exchangeable plates for Hectochelle. This system could be implemented by the Mexican partners, under technical advise from MMT and also from SDSS. With a well put proposal and a strong instrumentation team, we think it is possible to adapt the current system to the TSPM, so that the lifespan of the instrument, even if its efficiency is reduced by the requirement of positioning fibers by hand.
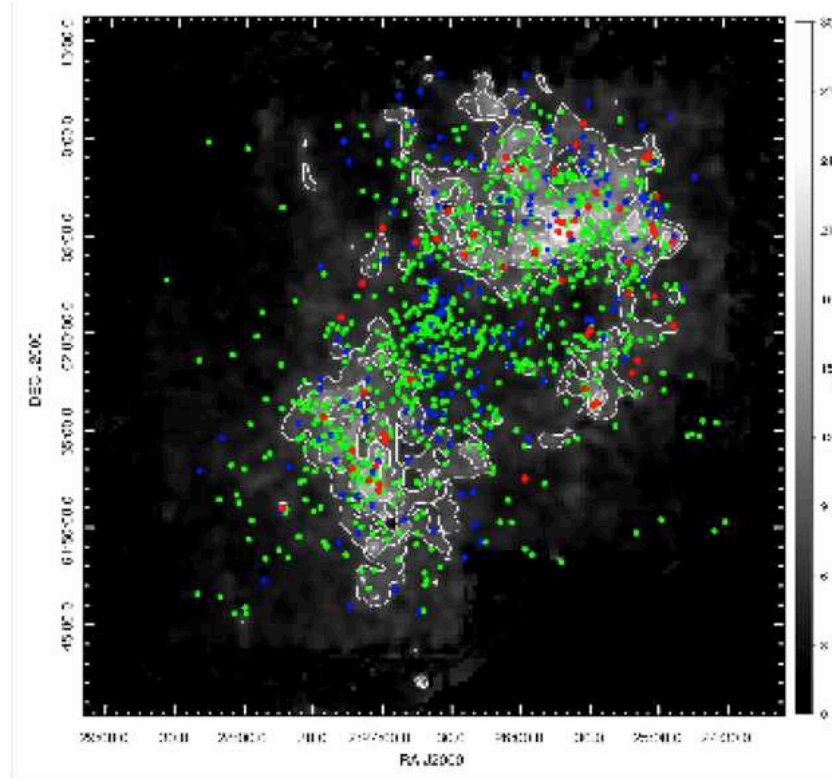
Fig. 1: Gray scale and contours show a dust extinction map of the W3 complex. Dot symbols indicate locations of candidate young star members at different evolutive stages (red: proto-stars, green: stars with prominent circumstellar disks, blue: stars with receding circumstellar disks).

2 3-D Structure of Molecular Gas in the Milky Way

Characterizing the structure of molecular clouds down to the scales of pre-stellar cores is key to understanding the initial conditions of star formation. The structure of molecular gas clouds is not easy to determine, as molecular Hydrogen (H2) cannot be observed directly because it lacks a permanent dipole moment and its rotational transitions are very weari-k. Molecular emission from tracers like CO used to be the preferred trace surrogates, and they work well for the inter-clump medium and the relative diffuse external layers of clouds, but they are severely depleted in the dense regions where stars form (Bergin et al. 2002). A more direct tracer is dust, which obscures clouds and comprises about 1% of the cloud mass. Dust can be fairly assumed to be uniformly dis- tributed in the gas (e.g. Whittet, 2003), and observations have shown that the column density is linearly dependent to the reddening of background stars by dust grains. At near-infrared wavelengths, clouds can be penetrated to reveal the background sources, each working as an individual measurement of reddening: By averaging stellar reddening within an aperture and scanning across a field, we can map the

variations of dust extinction across a cloud and construct maps of H2 column density with resolutions comparable of those obtained with radio telescopes. This Near-Infrared Color-Excess technique or NICE (Lada et al. 1994) became a practical way of using photometry in a minimum of two bands to map the structure of molecular clouds. The NICE technique was optimized as a multi-band technique (NICER) (Lombardi et al. 2001), has also recently been improved with complex noise reduction techniques (Lombardi et al. 2009) and can even include extragalactic sources as individual measurements of reddening by dust (Foster et al. 2008). The same technique has also been used to map extinction at unprecedented levels of $70 < A_V < 100$ visual magnitudes (Román-Zúñiga et al 2009). The color excess technique is thus ideal for the construction of deep, highly detailed two-dimensional maps of molecular clouds at a relatively low observational cost. Other methods, like the Raleigh-Jeans Color Excess (RJCE) technique (Majewski et al. 2011), which make use of multi-band catalogs that include Spitzer or WISE space telescopes photometry at 3.5-5 μm have been recently shown to map extinction at even more complex regions where dense and diffuse material is present.

Now, by combining accurate mapping of molecular clouds with increasing quality paralax measurements of foreground stars, it is possible to estimate distance to a cloud with precisions of the order of only tens of parsecs. Studies like those of Knude et al 2008, Lombardi et al (2008) and others, show how a simple Bayesian inference method can be applied to estimate distance-extinction relations at a given line of sight. The success of the GAIA mission will imply that parallax measurements will be improved by orders of magnitude in only a few years, and that the precision to estimate distances to a cloud will also be improved. Knude et al already shown how with relatively little effort, it could be possible to estimate distances even within a single cloud, and thus the door to tridimensional mapping of molecular complexes is already open. A wide-field near-IR detector like MMIRS at TSPM, with the quality of the SPM at infrared wavelengths to make imaging surveys, will surely allow the construction of exquisitely detailed maps of different molecular cloud complexes -the resolution of pre-stellar core scales willl depend of distance to the cloud and the density of background sources, but the uniformity of the map will be directly related to the depth and precision of the photometry-. If MMIRS or a similar instrument is not available, then MEGACAM could also do the trick: recent studies like those of Sale et al (2009) showed the feasibility of the Mapping Extinction Against Distance (MEAD) technique using data from the IPHAS survey (Drew et al 2005). The MEAD technique shows that optical colors from r, i and Hα photometry, plus parallaxes, can be used to construct distance-extinction relations of high precision. While less suitable for molecular clouds, these methods can be used to estimate the tri-dimensional structure of the molecular gas in the spiral arms of the galaxy. An instrument like MEGACAM at the TSPM could easily improve the IPHAS catalogs in quality and sensitivity and, in synergy with GAIA could provide fantastic insight into this problem.

3 References

Alves, J., Lombardi, M. & Lada, C. J. 2007, A&A, 462, L17
Bastian, N., Covey, K. R. & Meyer, M. R. 2010, Annu. Rev. Astro. Astrophys, 48, 339
Bergin, E. A., Alves, J., Huard, T. & Lada, C. J. 2002, ApJ, 570, L101
Covey, K. et al. "APOGEE-2 Young Cluster Science Requirements Document", Sloan Digital Sky Survey IV

de Grijs, R., Anders, P., Zackrisson, E. & Östlin, G. 2013, MNRAS, 431, 2917

Drew, J. E., Greimel, R., Irwin, M. J., et al. 2005, MNRAS, 362, 753-776

Foster, J. B., Roman-Zúñiga, C. G., Goodman, et al. 2008, ApJ, 674, 831

Foster, J., Cottaar, M., Covey, K. et al. 2015, ApJ, 799, 136

Fürész, G., Hartmann, L. W., Szentgyorgyi, A. H., et al. 2006, ApJ, 648, 1090

Fürész, G., Hartmann, L. W., Megeath, et al. 2008, ApJ, 676, 1109

Kissler-Patig, M., Jordán, A. & Bastian, N. 2006, A&A, 448, 1031

Knude, J. & Nielsen, A. S. 2001, A&A, 373, 714-719

Kruijssen, J. M. D., Maschberger, T., Moeckel, N., et al. 2012, MNRAS, 419, 841

Lada, C. J., Lada, E. A., Clemens, D. P. & Bally, J. 1994, ApJ, 429, 694

Lada, C. J. & Lada, E. A. 2003, Annu. Rev. Astro. Astrophys, 41, 57

Lombardi, M. & Alves, J. 2001, A&A, 377, 1023

Lombardi, M., Lada, C. J. & Alves, J. 2008, A&A, 480, 785

Lombardi, M. 2009, A&A, 493, 735

Majewski, S. R., Zasowski, G. & Nidever, D. L. 2011, ApJ, 739, 25

Roman-Zúñiga, C. G., Elston, R., Ferreira, B. & Lada, E. A. 2008, ApJ, 672, 861-887

Roman-Zúñiga, C. G., Lada, C. J. & Alves, J. F. 2009, ApJ, 704, 183

Román-Zúñiga, C. G., Ybarra, J., Megias G. et al. 2015, AJ (in press)

Sale, S. E., Drew, J. E., Unruh, Y. C., et al. 2009, MNRAS, 392, 497

Whittet, D. 2003, Dust in the galactic environment, IOP Publishing, 2003 Series in Astronomy and Astrophysics, ISBN 0750306246

Determination of presence of shocks caused by PNe halo-ISM interaction

JUAN LUIS VERBENA CONTRERAS

Instituto de Astronomía y Meteorología, Universidad de Guadalajara
Av. Vallarta 2602, Col. Arcos Vallarta Sur, C.P. 44130, Guadalajara, Jalisco, México

INSTRUMENT: BINOSPEC

1 Scientific Aim

A shock in a PNe causes the electronic temperature T_e to increase, which in turn causes an enhancement of the [OIII] emission. On the other hand, a decrease in the electronic density N_e will cause a decrease in the Hα emission (Guerrero et al. 2013). Because of this effects, we can search for evidence of shocks caused by the interaction between the ISM, and the outer envelope of PNe, which we can then model using hydordynamics simulations. In this project we want to search for shocks as evidence of interaction between the ISM and PNe halo. We are most interested in the Hα line at 6563.8Å, which is known to be a detectable line in the objects and regions of interest of this proposal, and the [OIII] line at 5007Å. The [OIII]/Hα ratio will give us evidence of shocks in the region. This emission is usually very weak in the halo, thus we are in need of a telescope sensitive enough as to reduce the integration time needed to achieve a decent signal to noise ratio. This sensitivity can be achieved with the 6.5 meter telescope.

2 Methodology

We will observe as may regions of each PN halo in as many directions as possible, where we expect to see different line ratios due to the direction of motion of the object with respect to the ISM and the shocks we expect to be caused by this.

The objects we plan to observe are the following:

Object	Right Ascention	Declination
Cn 1-5	18h 29m 11.659s	-31° 29' 59.16"
NGC 2438	07h 41m 50.51s	-14° 44' 07.7"

The choice of objects has been based on the coordinates, as well as the fact that we have photometry that suggests an enhancement in the H_α emission in the halo, as can be seen in the figure. We still don't have spectral information that will help us understand if we have shocks and thus interaction that we can model with a hydrodynamics code we have already produced.

Regarding the quantity of nights we request for this project, we'd like to have at least a couple of nights per object, to make sure we get a good signal to noise ratio that will give us confidence in then results and more robust data for our simulations. We have already tried to observe these lines with a 2m telescope, in the Guillermo Haro observatory, but the resulting signal to noise isn't satisfactory.
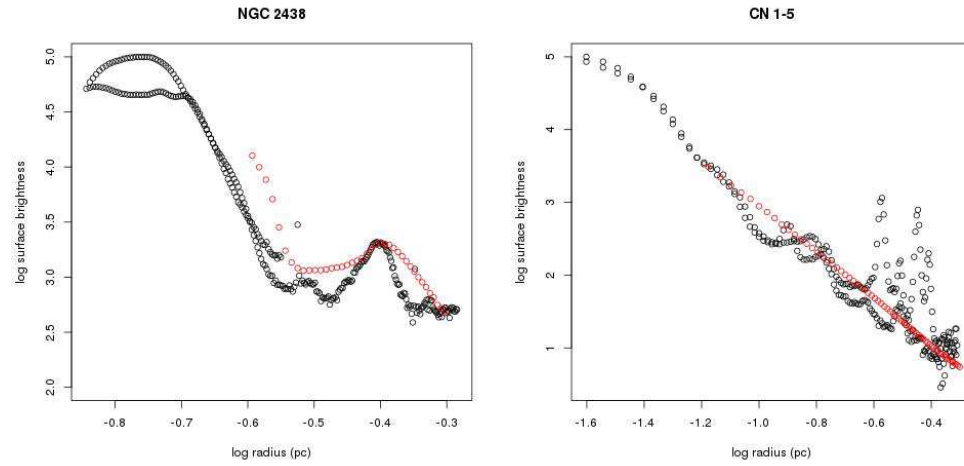

Fig. 1: NGC 2438 and CN 1-5. In red we show the modelling assuming no interaction and in black we show the actual observations.

References

Guerrero M.A., Toalá J.A., Medina J.J., Luridiana V., Miranda L.F., Riera A., Velázques P.F., 2013, A&A, 557, A121, 12

Part II
Extragalactic Astronomy

Star formation histories of galaxies in the local Universe using the resolved bright stars in the near infrared

Y. Divakara Mayya, Daniel Rosa Gonzalez, et al.

Instituto Nacional de Astrofísica, Óptica y Electrónica
Luis Enrique Erro 1, Tonantzintla, Puebla, México

Potential instrumentation: MMIRS + Megacam

1 Background

According to the currently popular hierarchical model of galaxy formation, galaxies grow by successive merging of low mass galaxies (Ellis & Silk 2007). On the other hand, in the classical monolithic collapse model, galaxies evolve by transforming their gas into stars at rates set by their initial masses. The predicted star formation histories (SFHs) are expected to be vastly different in the two scenarios: in the former case it is expected to be spiky, with each spike related to a merger event, whereas in the latter case, it is expected to be smooth. Hence, obtaining the SFH over the entire Hubble time has the potential to distinguish these two scenarios. The traditional method of determining SFHs using the Population Synthesis Techniques (Bruzual & Charlot 2003) has sensitivity only to the most dominant stellar population, and hence not useful in obtaining SFH over the entire Hubble time.

Resolved stellar populations are the best tracers of the SFH of a galactic region, and their color-magnitude diagram (CMD), the best tool to exploit the tracers (Tosi 2009). This is due to the well-established fact that the location of any individual star in a CMD is uniquely related to its mass, age and chemical composition. Thus from the CMD, we can directly obtain these parameters. In the case of simple stellar populations, i.e. coeval stars with the same chemical composition, isochrone fitting is the most frequently used method to infer the age of the system. In the case of galaxies, with rather complicated mixtures of different stellar generations, the diagram can be used to derive SFH, as illustrated in the left panel of Figure 1.

The technique of determination of SFH of external galaxies through the use of resolved stellar population is made possible through the unprecedented resolving power of the images obtained by the WFPC2 and ACS aboard the Hubble Space Telescope (HST). Since its launch almost 2 decades ago, SFHs are obtained for most of the *dwarf* galaxies in the local group (Tosi 2009), and also in the group of M81 (Weisz et al. 2008). However, study of *massive, high surface brightness* galaxies is crucial in order to understand galaxy formation. The ACS

Nearby Galaxy Survey Treasury (ANGST; Dalcanton 2008) project is aimed to do this in galaxies within a distance of 4 Mpc. Even with the HST resolution, crowding becomes an issue in the inner regions of nearby giant galaxies. In addition, there are only a handful of giant galaxies closer to 4 Mpc, making it necessary to look for techniques that can be used to investigate SFH of giant galaxies at distances greater than this. As will be discussed below, use of infrared bright stars in a near infrared (NIR) CMD promises to allow the determination of SFHs to distances up to 6 Mpc even using ground based telescopes. The increased volume over which the sample can be chosen gives a great opportunity to understand the formation of galaxies.

2 Star formation histories of nearby galaxies using TSPM

In recent years, several NIR surveys (i.e. DENIS, 2MASS, SAGE, and S3MC data for the Magellanic Clouds) have clearly demonstrated that the Thermally Pulsing Asymptotic Giant Branch (TP-AGB) stars account for most of the bright-infrared (IR) objects in resolved galaxies (Cioni et al. 1999; Bolatto et al. 2007). These red stars have the potential to facilitate the determination of the SFHs through the use of NIR CMDs, and theoretical isochrones (Marigo et al. 2008). An example of this for the resolved stars in the LMC is shown in Figure 1 (middle panel).

The following special properties make the NIR CMDs very useful for the study of SFH in nearby galaxies:

- *Identification of TP-AGB and Carbon stars:* Only stars that attain colors redder than $J - K > 1.3$ mag are the C-stars, which represent a short-lived phase in the TP-AGB evolution. These stars can be un-ambiguously identified among the population of resolved stars. Only stars of initial mass less than 7 M$\odot$ pass through the Carbon-rich phase of the AGB. The corresponding age of the stars is >200 Myr. Successively lower mass stars reach this phase at later times, and they are systematically fainter. Hence, the SFH can be derived by counting the relative number of stars in successive magnitude bins.
- *Detection from ground-based telescopes:* Detection of individual stars in galaxies depends on the contrast a star offers in the background of other stars. The main contributors to the background are the low-mass main sequence stars. At infrared wavelengths, the AGB stars are 5–10 mag brighter than the background stars, which facilitates their easy detection even with the ground-based telescopes. It may be noted that the horizontal branch (HB) stars, critical for the determination of SFH using the optical CMDs, are only 2–3 mag brighter than the stars that make up the background, and hence it is necessary to resolve the background-contributing population for their detection.
- *The time-resolution and the look-back times of the derived SFH:* The TP-AGB stars span a limited range of magnitudes ($\sim$3) in the K-band, with the brightest stars reaching $M_K = -10$. The faintest of the TP-AGB stars have $M_K = -7$ mag, which are associated with stellar populations as old as 10 Gyr. Observations that can detect stars of $M_K = -7$ mag can infer the SFHs all the way up to the Hubble time. The time resolution of the SFH depends on the size of the magnitude bin. For magnitude bins of around 0.2 mag, one can hope to achieve time resolutions of $\sim$1 Gyr for look back times greater than a gigayear and much better at earlier epochs. This compares favorably with what is possible these days for
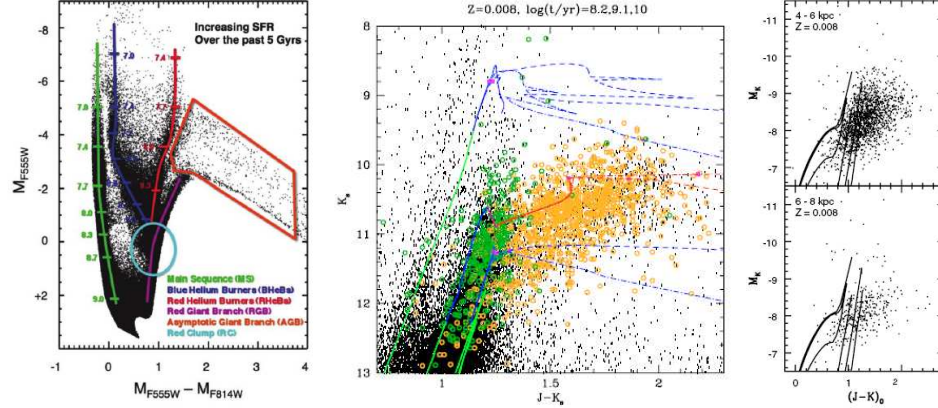
Fig. 1: (left) Illustration of determination of SFH using CMDs from Weisz et al. (2008). The plot shows a simulated CMD of increasing SF over the past 5 Gyr. Important features on the CMD are highlighted. The logarithmic ages of stars are overlaid for the main sequence, blue Helium burners and red Helium burners. (middle) Comparison of recent isochrones of Marigo et al. (2008) with the data for the LMC. Three sets of isochrones at log ages (in yr) 8.2, 9.1 and 10.0 are shown (brighter at smaller ages) for two different prescriptions of circmumstellar dust. The symbols show spectroscopically confirmed M (green) and C-stars (orange). (right) Illustration of obtaining SFH using CMDs in M82 disk from Davidge (2008). The two plots show the CMDs for the stars detected at two consecutive radial bins. The plotted isochrones correspond to log ages (in yr) 7.5, 8.0, 8.5 and 9.0 from Girardi et al. (2002; 2004). These tracks do not include the C-star phase during which $J - K$ colors become redder than 1.3 mag. By a comparison of the $J - K$ colors of M82 and LMC stars, it can be inferred that many of the detected stars in M82 are C-stars.

galaxies in the local group using HST-derived optical CMDs. $M_K = -7$ mag corresponds to $K = 22$ at a distance of 6 Mpc. TSPM, in combination with a NIR instrument such as MMIRS will be able to reach these limiting magnitudes with net exposure times of 2 hours. Hence, TSPM/MMIRS combination promises to obtain the SFH spanning the entire Hubble time for all galaxies that are nearer than 6 Mpc.

2.1 Illustration of SFH through NIR CMD in the nearby galaxy M82

An insight of what can be achieved with TSPM/MMIRS can be obtained from a study of the nearby high surface brightness galaxy M82 by Davidge (2008) (see Figure 1). All the bright stars detected in the disk of M82 from deep images obtained with WIRCAM at CFHT are plotted. Stars with $J - K > 1.3$ mag in this diagram are C-stars of ages between 0.1 to 1 Gyr. More importantly the CMD rules out the existence of stars younger than 0.1 Gyr, consistent with a disk-wide burst model for this galaxy proposed by Mayya et al. (2006). The observations had a 50% completeness limit up to K=20 ($M_K \approx -8$), with a net exposure time of 40 minutes. By going down by 1 mag for this galaxy, one could definitely establish

the SFH over the entire Hubble time. With TSPM, it would be possible to do that in only a few minutes of observing time. M82 is located in the M81 group at a distance of 3.6 Mpc (distance modulus of 27.8 mag). TSPM will allow similar studies to be carried out up to a distance of ~ 6 Mpc. The increased volume would allow the SFHs to be determined in several massive galaxies, thus providing the key to understand the galaxy formation.

References

Bolatto, A.D., Simon, J.D., Stanimirovic, S. et al. 2007, ApJ, 655, 212
Bruzual, G. & Charlot, S. 2003, MNRAS, 344, 1000
Cioni, M.-R.L., Girardi, L., Marigo, P., & Habing, H. J. 2006, A&A, 448, 77
Dalcanton, J. 2008, in Galaxies in the Local Volume, ed. B. S. Koribalski & H. Jerjen, Astrophysics and Space Science Proceedings (Springer)
Davidge, T. J. 2008, ApJ, 136, 2502
Ellis, R. & Silk, J. 2007 astro-ph/0712.2865
Girardi, L., Bertelli, G., Bressan, A., et al. 2002, A&A, 391, 195
Girardi, L., Grebel, E.K., Odenkirchen, M. & Chiosi, C. 2004, A&A, 422, 205
Mayya, Y.D., Bressan, A., Carrasco, L., & Hernandez-Martinez, L. 2006, ApJ, 649, 172
Tosi, M. 2009 astro-ph/0901.1090
Weisz, D. et al. 2008, ApJ, 689, 160

H$_2$ETGs: tracing accretion/SF/feedback in early-type galaxies with TSPM

OLGA VEGA ET AL.

Instituto Nacional de Astrofísica, Óptica y Electrónica
Luis Enrique Erro 1, Tonantzintla, Puebla, México

POTENTIAL INSTRUMENTATION: MMIRS + ATLAS

COLLABORATORS:
R. Rampazzo (OAPD, Italy), A. Bressan(SISSA, Italy), M. Clemens (OAPD, Italy), D. Rosa-González (INAOE), M. Chávez (INAOE), P. Panuzzo (CNRS, France), M. Mapelli (OAPD, Italy).

1 Introduction

Early type galaxies (ETGs) have long been considered to be inert, red and dead stellar systems, essentially devoid of gas and dust. This view is radically changed since a number of imaging and spectroscopic studies have revealed the presence of a multiphase interstellar medium (ISM). Starting with the pioneering work of Phillips et al. (1986), optical spectroscopic studies have revealed that the emission line ratios in ETGs are typical of Low-Ionization Nuclear Emission-line Regions (LINERs, Heckman 1980). However, after about three decades of studies, there is still strong debate about the excitation mechanism in LINERs. The three most viable mechanisms are: a) low accretion-rate AGN (e.g. Kewley et al. 2006; Ho 2009); b) photoionization by old, post-asymptotic giant branch (PAGB) stars (e.g. Trinchieri & di Serego Alighieri, 1991; Binette et al. 1994; Stasinska et al. 2008; Sarzi et al. 2010; Capetti & Baldi 2011); c) shocks (e.g. Koski & Osterbrock 1976; Dopita & Sutherland 1995; Allen et al. 2008).

In the study of the optical emission lines in a sample of 65 ETGs, Annibali et al. (2010) have demonstrated that optical diagnostic diagrams (e.g., [OIII]/Hβ vs [NII]/Hα) can not discriminate between low accretion-rate AGNs and shocks, moreover Annibali et al. show that PAGB stars can explain only the observed nuclear emission in the 22% (the fainter tail) of the studied LINERs.

The mid infrared (MIR) window adds new clues to the ETGs/LINERs investigation and in principle it is able to well separate LINERs powered by SF (9% have class-3 spectra in RSA). Vega et al. (2010), Panuzzo et al. (2011), and Rampazzo et al. (2013) shown that the
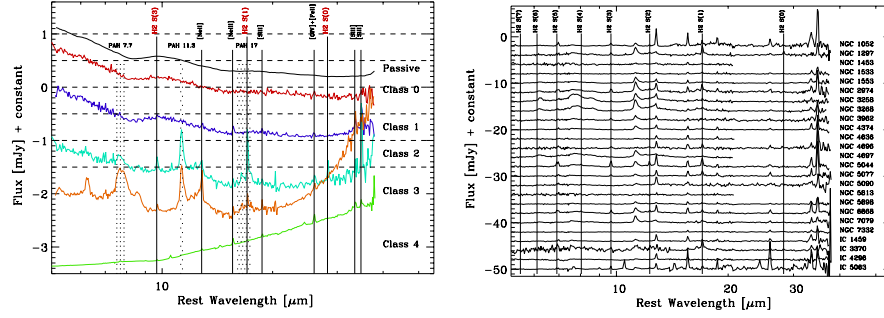
Fig. 1: *Left panel*: MIR spectra of ETGs representative of the five classes defined in Panuzzo et al (2011). The thicker black lines mark the positions of the main H2 rotational lines. *Right panel*:Spitzer-IRS spectrum of some H2ETGs in our sample.

MIR-spectra of ETGs fall into five MIR classes (see left panel in Figure 1), ranging from AGN (class-4), star forming (SF) nuclei (class-3, lines + PAHs with normal ratios), transition class-2 (lines + PAHs with anomalous ratio), class-1 (lines, no-PAHs) to passively evolving nuclei (class-0, no PAH, no emission lines).

Demographic studies of the morphology and kinematics, presence of dust-lanes and emission from radio to X-ray, supports the view that the MIR classes are connected to a recent accretion episode. Each MIR class may represent a snapshot of the evolution in the inner regions of the ETGs/LINERs, starting from, and ending with a passively evolving (MIR class-0) spectrum (see Fig.11 in Panuzzo et al. 2011).

One interesting result from this analysis in the extremely intense H2 emission found in ETGs (34 % of Es and 51% of S0s in RSA, see right panel in Fig. 1). Most of them are LINERS and show anomalous low 7.7μm/11.3μgm PAH ratio, indicating that the emission is not powered by star formation (Vega et al. 2010), i.e. only a small fraction of H2 bright ETGs (H2ETGs) are excited via UV fluorescence in photo-dissociation regions (PDRs). Other proposed excitation mechanisms of H2 are X-ray illumination (e.g. Maloney 1996) and shocks (e.g. Hollenbach & McKee 1989; Vega et al. 2010). Some studies suggest that neither diffuse X-ray emission (see e.g. Roussel et al. 2007) nor X-ray illumination from AGN (see e.g. Ogle et al. 2010) are efficient enough to produce the large observed H2 emission. The [NeIII]15.5/[NeII]12.8μm vs [SIII]33.5/[SiII]34.8μm MIR diagnostic diagram shows that H2ETGs fall in the shock regions (Panuzzo et al. 2011). However, a degeneracy persists with the AGN models if a spread in the dust content of the narrow-line region is allowed. Jet and accretion driven flows are both viable mechanisms to produce shocks in LINERs (Dopita & Sutherland 1995; Nagar et al 2001; Dopita et al.1997; Crawford & Fabian 1992) as well as turbulent motions of gas clouds within the potential well of the galaxy (Ho 2009; Annibali et al. 2010 and references therein). Shocks may also be due to supernova remnants or outflows in a region where a starburst has occurred (see van der Werf 2000). Figure 2 shows our total sample of H2ETGs compared with other nearby galaxies showing H2 emission: it is evident the difficulty in discriminating among various mechanisms of excitation at work from such diagnostic diagrams. Moreover, radically different 2D geometries of the H2 emission are expected in the case of PDR, shocks or AGN excitation mechanisms (e.g. Donahue et al. 2000).
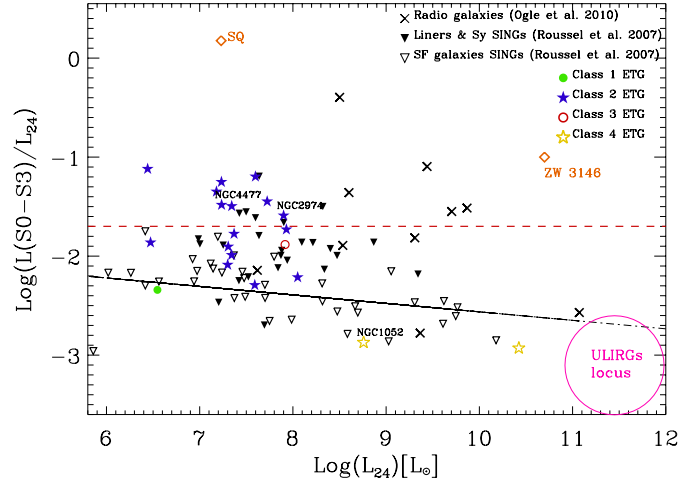
Fig. 2: Ratio of the pure rotational H2 emission lines luminosity to the IR luminosity at 24μm. Our H2ETGs (stars, belonging to different MIR classes) are shown in comparison with radio (Ogle et al. 2010,), LINERs, Sy and SINGs Star Forming galaxies in (Roussel et al. 2007) and the Stefan's Quintet (SQ) intergalactic shock (Cluver et al. 2010). Some objects in class-2 (NGC 4477 and NGC 2974) and in class-4 (NGC 1052) are indicated. Class-3 ETGs lie among star forming SINGs spirals. The dashed (red) line separates normal H2 emission from MOHEG (MOlecular Hydrogen Emission-line Galaxies). The latter have a high H2/7.7 PAH ratio (> 0.04), implying an excitation not fully justify by a pure UV heating (Ogle et al 2010). The solid (black) line is the fit of Star Forming galaxies. Different powering mechanisms are at work in the nuclei of H2ETGs, that can be disentangled via the morphological study of H2 emission and the study of gas kinematics.

The proposed spectroscopic study between 1.25-2.45 μm will allow to detect not only the H2 line (2.122μm) but also the [FeII]1.644μm and the Brγ 2.16 μm emission lines. The [FeII]1.64μm line is favored in zones of partially ionized gas which are large when the gas is heated by X-rays (power-law photoionization) or by shocks (Mouri et al. 2000). The [FeII]1.64/Brγ ratio is typically a factor ~ 50 higher in shocked regions than in AGNs (see models by Allen et al. 2008 and Groves et al. 2004). Thus a measure of that ratio will allow us to separate shock regions from regions where AGN photoionization dominate. Therefore, to directly investigate the different mechanisms for the excitation of H2, high resolution NIR-H2 narrow-band imaging and NIR spectroscopy are the most suitable observations.

We foresee to use these data-set to constrain our chemo-photometric smoothed-particle hydrodynamics (SPH) simulations providing the global evolution of these ETGs in a fully consistent picture (e.g. Mazzei et al. 2014 and references therein). We also simulate the (thermo)dynamical evolution of molecular clouds in the nuclei of our host ETGs to study the properties of shocks. MMIRS at the TSPM or Atlas at MMT could be suitable instruments to carry out the spectroscopic part of this investigation. We would also request narrow band H2 filters to observe the different H2 emission geometries needed in this work.

Summary

We suggest that MIR classes mark evolutionary phases during an accretion episode that may induce SF, and/or AGN activity/feedback. H2ETGs and a large fraction of nearby LINERS may represent the final (cooling) phases before the galaxy came back to a passive evolution. Optical diagnostic diagrams alone are unable to disentangle mechanisms at work and 2D studies are rare. The high resolution H2 images plus spectroscopic information accurately modeled will allow us to disentangle the gas powering mechanism/s (shock, AGN, SF) and their interplay as drivers of the evolution in ETGs/LINERs.

References

Allen et al. 2008, ApJS, 178, 20
Annibali et al. 2010, *A&A* 519, A40
Binette et al. 1994, *A&A*, 292, 13
Capetti & Baldi 2011, arXiv:1103.3652
Cluver et al. 2010,ApJ, 710, 248
Crawford & Fabian 1992, MNRAS, 259, 265
Donahue et al. 2000, ApJ, 545, 670
Dopita & Sutherland 1995, ApJ, 455, 468
Dopita et al.1997, ApJ, 490, 202
Groves et al. 2004, ApJS, 153, 9
Heckman 1980, *A&A*, 87, 152
Ho 2009, ApJ, 699, 626
Ho 2009, ASR, 23, 813
Hollenbach & McKee 1989, ApJ, 342, 306
Kewley et al 2006, MNRAS, 372, 961
Koski & Osterbrock 1976, ApJL, 203, L49
Mazzei et al. 2014, ASR, 53, 950
Maloney 1996, ApJ, 466, 561
Mouri et al. 2000, ApJ, 528, 186
Nagar et al 2001, ApJL, 559, L87
Ogle et al. 2010, ApJ, 724, 1193
Panuzzo et al. 2011, A&A, 528,10
Phillips et al. 1986, AJ, 91,1062
Rampazzo et al. 2013, MNRAS, 432,364
Roussel et al. 2007, ApJ, 669, 959
Sarzi et al. 2010, MNRAS, 402, 2187
Stasinska et al. 2008, MNRAS, 391, L29
Trinchieri & di Serego Alighieri, 1991, AJ, 101, 1647
van der Werf 2000, in Molecular Hydrogen in Space eds. F. Combes & G. Pineau des For.ets, Cambridge Univ. Press
Vega et al. 2010, ApJ, 721,1090

Part III
Cosmology

Peculiar velocities of clusters and groups of galaxies inside large scale structures

César A. Caretta, Marcel Chow-Martínez and Heinz Andernach

Departamento de Astronomía, DCNyE-CGT, Universidad de Guanajuato
Apartado Postal 144, C.P. 36000, Guanajuato, Gto., México

Potential instrumentation: MMIRS + Binospec

1 Introduction

The biggest coherent structures in the Universe are the superclusters of galaxies. By coherent one means, in such a context, that these large scale structures are expected to be gravitationally bound, hosting some virialized structures (like some galaxy cluster cores), but overall in a dynamically young state, perhaps even still expanding with the Hubble flow, albeit at a decelerated rate. This implies that the superclusters of galaxies still preserve the memory of their formation, in such a way that the study of their structure, internal dynamics and composition may give important clues about the evolution of the Large Scale Structure of the Universe. Bulk flows have already been measured for the Local Supercluster surroundings (e.g. Dressler et al. 1987; Hudson 1993; Lavaux et al. 2010; Pomarede et al. 2013, Tully et al. 2013), which made possible to measure, for example, our motion towards the "Great Attractor" (e.g. Lynden-Bell et al. 1988), and also streaming motions of individual groups and clusters (e.g. Bernardi et al. 2002; Hudson et al. 2004; Springob et al. 2007; Mutabazi et al. 2014). On the other hand, very few Abell clusters, which are members of superclusters in the Local Universe, have distance estimates for a number of individual galaxies. In this project we intend to study the internal dynamics and evolution of nearby ($z \leq 0.05$) superclusters of galaxies by measuring peculiar radial velocities for the clusters, substructures and groups of galaxies they host. In order to obtain peculiar motion of these systems we need first to measure directly the distance for a certain number of individual member galaxies, by using methods such as the Tully-Fisher and Fundamental Plane relations. With these distances we can estimate the mean Hubble flow velocity of their systems and, by combining this information with radial velocity data we can calculate their peculiar motion.

The steps for this challenging work are:

1. identify the clusters and groups of galaxies that compose the superclusters of galaxies;
2. study the internal structure and galaxy membership for each cluster, substructure and group of the sample;

3. check the literature for existing data for such member galaxies (direct distance measurements, spectroscopically measured radial velocities, photometric data on luminosities, diameters, etc., and spectroscopic data on central stellar velocity dispersions or maximum rotation velocities);
4. select unobserved member galaxies, in a number enough for completing the individual cluster/groups subsamples in order to measure their peculiar velocities to an acceptable level of uncertainties;
5. obtain the complementary photometric and spectroscopic data for these unobserved member galaxies;
6. calculate the peculiar radial velocity for each system (cluster, substructure and group);
7. study the internal dynamics of each supercluster of the sample.

The state of art of such endeavor is:

1. We have already selected the superclusters of galaxies and their member clusters and groups (e.g. Chow-Martínez et al. 2014).
2. We have advanced on the study of the internal structure and membership for some of the member clusters and groups (Caretta et al., in preparation).
3. There are already some data available on direct distance measurements for galaxies in the Local Universe (e.g. Springob et al. 2007; Tully et al. 2013; Campbell et al. 2014), and many databases with photometric and spectroscopic data for galaxies that are in our subsamples of cluster/group members.
4. We have already estimated the number of individual member galaxies we need for each system in order to obtain a reliable estimation of its peculiar velocity. We have also selected some target samples that need new photometric and spectroscopic observations.

2 Proposed methodology

For achieving an adequate level of photometric quality and signal to noise, deeper enough for covering the subsamples we have selected in a reasonable amount of time, we need a mediumlarge telescope, like the 6.5m telescope planned for San Pedro Mártir Observatory, and an instrument with both photometry and spectroscopy capability. Optical and/or NIR may be used both for photometry and spectroscopy, the first with de advantage of been already widely used for photometric parameters and line widths, while the second allows, as have been pointed in the last decades, sharper distance relations (taking advantage of the smaller k-corrections and interstellar extinction together with the more direct connection with the stellar component of galaxies). An adequate instrument, for example, is the MMIRS. Usually the targeted galaxies are among the 30 brightest members of each cluster/group, and cover a magnitud range between 9 and 15 in the H band. A 30' FOV is ideal for covering even the brightest galaxies of the sample with enough field for measuring their background. For spectroscopy an intermediate resolution is needed for measuring the line strengths of relatively bright lines.

References

Bernardi, M., Alonso, M.V., da Costa, L.N., Willmer, C.N.A., Wegner, G., Pellegrini, P.S., Rité, C., Maia, M.A.G.; 2002, AJ, 123, 2159

Campbell, L.A., Lucey, J.R., Colless, M., Jones, D.H., Springob, C.M., Magoulas, C., Proctor, R.N., Mould, J.R., Read, M.A., Brough, S., Jarret, T., Merson, A.I., Lah, P., Beutler, F., Cluver, M.E., Parker, Q.A.; 2014, MNRAS, 443, 1231

Chow-Martínez, M., Andernach, H., Caretta, C.A., Trejo-Alonso, J.; 2014, MNRAS 445, 4073

Dressler, A., Faber, S.M., Burstein, D., Davies, R.L., Lynden-Bell, D., Terlevich, R.J., Wegner, G.; 1987, ApJ, 313L, 37

Hudson, M.J.; 1993, MNRAS, 265, 72

Hudson, M.J., Smith, R.J., Lucey, J.R., Branchini, E.; 2004, MNRAS, 352, 61

Lavaux, G., Tully, R.B., Mohayaee, R. Colombi, S.; 2010, ApJ, 709, 483

Lynden-Bell, D., Faber, S.M., Burstein, D., Davies, R.L., Dressler, A., Terlevich, R.J., Wegner, G.; 1988, ApJ, 326, 19

Mutabazi, T., Blyth, S.L., Woudt, P.A., Lucey, J.R., Jarrett, T.H., Bilicki, M., Schr oder, A.C., Moore, S.A.W.; 2014, MNRAS, 439, 3666

Pomarede, D., Courtois, H., Tully, R.B.; 2013, IAUS, 289, 323

Springob, C.M., Masters, K.L., Haynes, M.P., Giovanelli, R., Marinoni, C.; 2007, ApJS, 172, 599

Tully, R. B., Courtois, H.M., Dolphin, A.E., Fisher, J.R., H eraudeau, P., Jacobs, B.A., Karachentsev, I.D., Makarov, D., Makarova, L., Mitronova, S., Rizzi, L., Shaya, E.J., Sorce, J.G., Wu, P.; 2013, AJ, 146, 86

Tully, R.B., Courtois, H., Hoffman, Y., Pomarede, D.; 2014, Nature, 513, 71

The evolving Universe of quasars

Deborah Dultzin Kessler

Instituto de Astronomía, IA-CU, Universidad Nacional Autónoma de México
Circuito de la Investigación Científica s/n, Ciudad Universitaria, Del. Coyoacán, C.P. 04510, México, D.F.

Potential instrumentation: Binospec, MMIRS

1 Scientific context

Several ongoing and planned surveys will provide an unprecedented wealth of distant type-1 quasar samples, boosting the population of known quasars at $i \approx 21.5 - 22$, and even reaching down to $i \approx 26$ (see e.g. reviews in Chapter 8 of D'Onofrio et al.). Do we need to study more quasars and especially faint quasar at high redshift? The answer is a strong yes.

At low redshift, quasar UV, optical and IR rest-frame properties are not simply scattering randomly around an average but can be organised along a sequence that is conceptually analogous to the stellar main sequence in the H-R diagram (the so-called Eigenvector 1 sequence, Boroson & Green 1992; Sulentic, Marziani, & Dultzin-Hacyan 2000; Shen & Ho 2014). The main governing parameters are thought to be luminosity-to-black hole mass ratio (L/M) along with black hole mass and viewing angle. Black hole spin and gas metal contents are also playing an important role. Estimating these parameters for each individual quasar requires high S/N and intermediate dispersion spectroscopy (spectral resolution $\approx$1000 and continuum S/N > 20; i.e., Sulentic et al., 2014).

At high redshift, we expect to find quasar populations with significantly different properties. Even the deepest present-day survey provide a biased view of quasar populations. Fig. 1 shows that a flux limit introduces a strong selection effect on quasar sampling for a fixed absolute magnitude range (left) as well as on a key physical parameter like Eddington ratio (right). Current studies infer a down-sizing in black hole growth, but we actually know very little (if anything) of any small black hole mass population of quasars at high z.

The ongoing optical and IR surveys will provide the identification of quasars that will still need intermediate resolution high S/N spectra for a quantitative empirical parameterisation, a proper contextualisation within the Eigenvector 1 sequence as well as within a physical parameter space that includes M, Eddington ratio, orientation metallicity, etc. The availability of a large aperture telescope of the 6 m class is vital to this endeavour. If performing like GTC OSIRIS, Binospec will allow high S/N observations ($\geq$ 20) in the rest frame UV of quasars
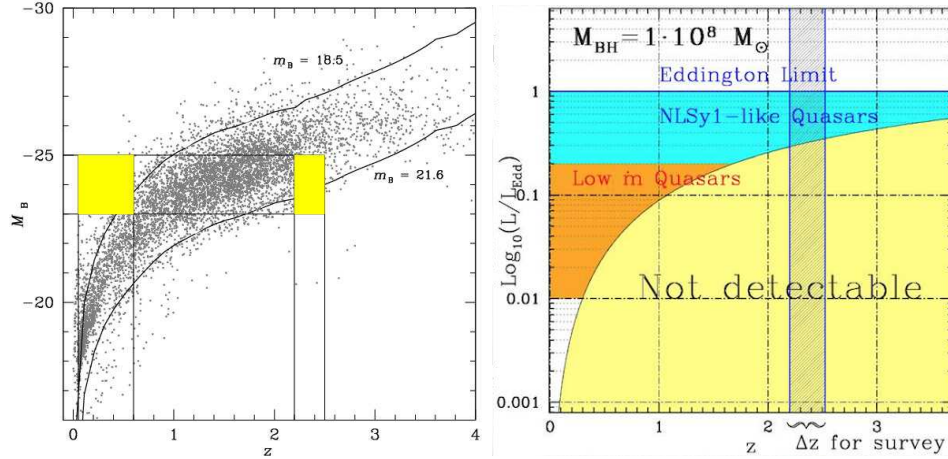
Fig. 1: *Left*: Bias in sampling of quasars for a fixed absolute magnitude range, in the local Universe and in an hypothetical pencil beam quasar survey in the z range $2.2 - 2.5$. At low z, the absolute magnitude range -23 to -25 includes the most luminous quasars. At high z, in the same absolute magnitude range there is a loss of sources at the faint end dues to the magnitude limit at 21.6: fainter quasars are not yet discovered. *Right*: Eddington ratio as a function of redshift, with the area of undetectable sources below a limiting magnitude $m_B \sim 21.5$ colored yellow. The redshift range of an hypothetical pencil beam quasar survey is identified by a dashed strip. From Sulentic et al. 2014.

in the redshift range $1.5 < z < 4$. Considering an expected quasar surface density at $g < 22$, $50 - 100$ quasars per square degree, some multiplexing advantage will be offered by the field-of-view ≈ 0.03 square degrees (i.e., up to 3 quasars per fields could be simultaneously observed). A great wealth of physical information can be extracted from the Hbeta spectral range: source placement in the Eigenvector 1 sequence, reliable estimates of BH mass from the Hbeta line profile, L/M (Eddington) ratio). The IR spectrometer MMIRS will allow to cover Hbeta up to K band i.e., up to redshift 3.8.

High S/N observations of faint quasars are instrumental to unbiased studies of black hole mass and accretion rate evolution, as well as gas chemical enrichment history in the host galaxies. Understanding quasar evolution is also a necessary step to build a satisfactory scenario of structure evolution in the Universe. Quasar mass outflows and radiation forces (whose prominence is a function of the quasar location in the Eigenvector 1 sequence) are expected to produce a strong effect on the host gas content, star formation rates as well as on its structure and dynamics (e.g. Fabian 2012).

2 Quasars for cosmology

Quasars radiating close to the Eddington limit (hereafter referred to also as extreme quasars) show distinguishing spectral properties that can be recognised in major surveys. Our research group developed a particular approach based on the Eigenvector 1 of quasars that enabled us
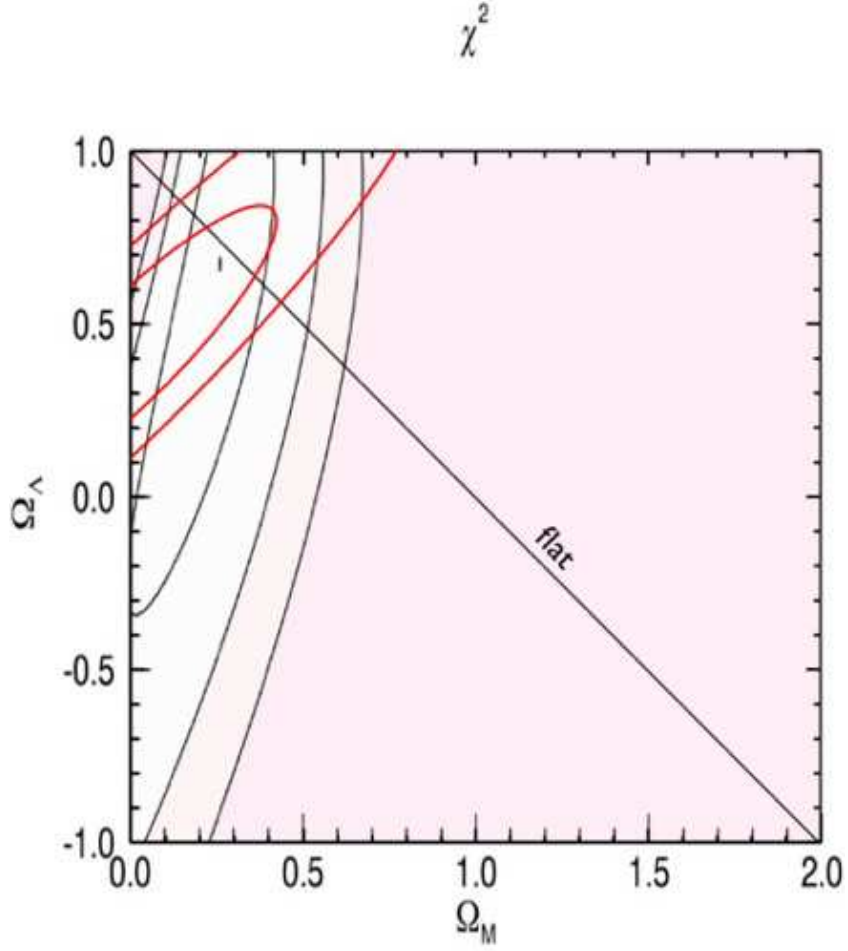
Fig. 2: Constraints set by the supernova photometric survey described by Campbell et al. 2013, ApJ, 763, 88 (black filled lines show confidence intervals are at 1 and 2σ)and by a mock sample (red; 1, 2, 3 σ). Only statistical errors are included in both cases.

to identify and isolate extreme accretors with Eddington ratio (proportional to the luminosity-to-mass ratio) close to 1 once an optical or UV rest-frame spectrum is available (Marziani & Sulentic 2014). If the Eddington ratio is known, it is then possible to derive distance-independent luminosities by computing the black hole mass. Extreme quasars with $z < 3 - 4$ might be used as "Eddington ratio standard candles". This possibility gave rise to a fledgling but booming field of research: several major papers in the past 2 years stressed the possibility of using extreme quasars as distance indicators (among them, Wang et al. 2013; La Franca et al. 2014).

Extreme quasars offer the non-negligible advantage that they can be found in large numbers. Their redshift distribution can be made statistically unbiased up to $z \sim 3 - 4$, where the most reliable distance indicators are not available and the effects of the energy density

of matter is dominant. The assessment of systematic effects will lead to a fully independent measure of Ω_M, will permit to significantly constrain Ω_Λ, and will offer the possibility of studying the cosmic evolution of the equation of state of dark energy. Expected constraints on Ω_M from a sample of 400 quasars, compared to a recent supernova survey, are shown in the Figure. Much larger samples ($\geq$1000 sources) can be pre-selected from low signal to noise spectra.

Dedicated observations in the optical and NIR with a large aperture telescope are needed to define the spectral energy distributions and emission line properties of highly accreting quasars, and to measure virial line widths to derive black hole masses. Extreme quasars occupy a very well defined place in the so-called quasar Eigenvector 1 sequence (Marziani & Sulentic 2014), but intrinsic dispersion in physical properties of these sources and eventual trends with redshift and luminosity have to be precisely known if these source are to be used as distance indicators. Binospec and MMIRS would provide suitable measurements for highly accreting quasars up to $z \sim 4$.

Current issues go beyond the existence of the dark energy and focus more on its properties. The simplest model for dark energy is a cosmological constant with a fixed equation of state ($p = w\rho$, with fixed $w = -1$). However, the dark energy density may depend weakly upon time, according to many proposed models of its nature (Carroll, S. 2005): a general scalar field predicts w to be negative and evolving with redshift. The ability to build the Hubble diagram uniformly covering a broad z range makes highly accreting quasars suitable probes for testing whether the dark energy equation of state is constant or is evolving as a function of redshift (following e.g., Piedipalumbo, E., et al. 2014; Capozziello S., et al. 2011).

References

Boroson & Green 1992, ApJS 80, 109
Capozziello S., et al. 2011, Phys.Rev. D84 124061
Carroll, S. 2005, ASP CS, 339, 4
D'Onofrio, Marziani, Sulentic, 50 years of quasars, Berlin:Springer
Fabian 2012, ARA&Ap 50, 455
La Franca et al. 2014, ApJ, 787, L12
Marziani & Sulentic 2014, MNRAS 442, 1211
Piedipalumbo, E., et al. 2014, MNRAS, 441, 3643
Shen & Ho 2014, Nat 513, 210
Sulentic, Marziani, & Dultzin-Hacyan 2000, ARevA&Ap, 80, 521
Sulentic et al., 2014, A&Ap, 570, A96
Wang et al. 2013, PhRev Lett., 110, 1301

The formation and evolution of cD galaxies

Simon N. Kemp et al.

Instituto de Astronomía y Meteorología, Universidad de Guadalajara
Av. Vallarta 2602, Col. Arcos Vallarta Sur, C.P. 44130, Guadalajara, Jalisco, México

Potential instrumentation: Megacam + Binospec

Collaborators:
E. Pérez-Hernández (IAM, U. Innsbruck), J.J. González (UNAM-DF), V.H. Ramírez-Siordia (IAM, UNAM-CRyA), A. Nigoche (IAM).

This is a project that will take advantage of the sensitivity of the TSPM 6.5m telescope to faint haloes of giant galaxies to investigate mechanisms of formation and evolution of these galaxies and compare with current ideas of galaxy formation and evolution, usually involving the hierarchical assembly of structures (e.g. Ascaso et al. 2014, Cooper et al. 2014) cD galaxies are supergiant elliptical galaxies found usually in the centres of rich clusters. They have an extended halo-like component (envelope) and an underlying de Vaucouleurs-Sérsic elliptical galaxy-like component. The envelope can reach radial distances of < 500 kpc (Oemler 1976, Schombert 1988). There have been many theories to explain the formation of these envelopes. These include tidal stripping (Gallagher & Ostriker 1972), where material is stripped from neighbouring galaxies in the cluster, falling into the gravitational potential of the cD; mergers, where the envelope is built up hierarchically by successive major and minor mergers with cluster galaxies; primordial origin (Merritt 1984), where the envelope is formed simultaneously with the rest of the elliptical galaxy (which appears to be related to recent theories of 'downsizing' (Neistein et al. 2006) and early formation of the largest galaxies); and cooling flows (Fabian et al. 1982), clusters with X-ray emission from hot gas frequently have a minimum in temperature in the centre which can be interpreted as a flow of cooling gas towards the central regions, and if the gas cools sufficiently it could form stars, and hence form the envelope populations.

The colours of the stars in the envelopes will be affected by their process of formation and subsequent evolution. We carried out a programme of deep surface photometry on a sample of 10 cD envelopes using the 2.1m and 1.5m telescopes at San Pedro Mártir, Baja California, México, obtaining 30-90 min total exposure per filter. For the majority of the galaxies we obtained very flat colour profiles within the errors, varying by no more than +/- 0.1 mag in $B - V$ (Kemp et al. 2009).The flat profiles imply similar stellar populations in the underlying galaxy and the envelope, maybe formed at the same time. This could favour the primordial origin or downsizing hypothesis, and implies that any subsequent evolution that the galaxy experiences does not usually dominate its global colours.
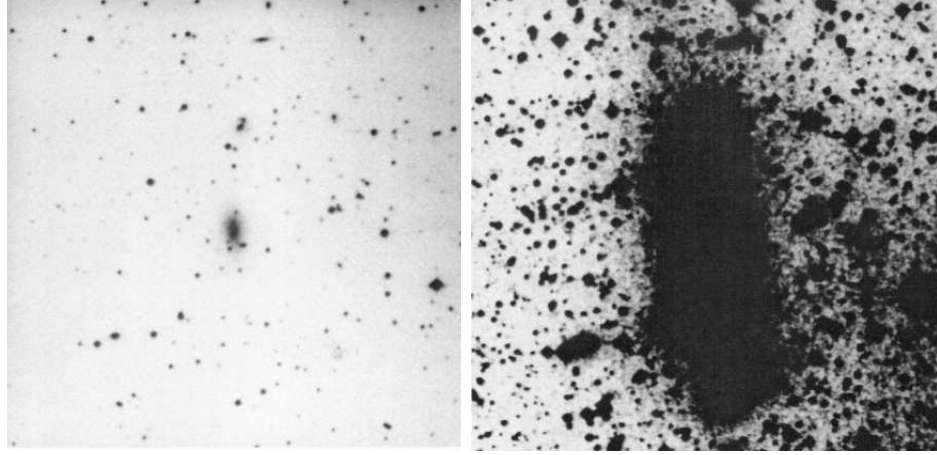
Fig. 1: The cD in Abell 3571 at low and high contrast (12 x 12 arcmin field)

Variations in age and metallicity of the stellar populations with position could produce similar colours. We have carried out a programme of medium-resolution spectroscopy of cDs at the 2.1m in San Pedro Mártir to obtain age and metallicity of stellar populations of our cD sample. We obtained spectra of the central regions of each galaxy and various radial positions along the slit up to r_e (Pérez-Hernández 2014), but with an adequate S/N only until the interface between the underlying elliptical and envelope. In general galaxies with flat red colour profiles have old populations of near-solar metallicity though there are exceptions (A2589 has young populations 2–6 Gyr in all positions with metallicity of 0.3–0.4, in spite of also having a flat, red, colour profile) while A2199 has younger ages at larger radii corresponding to the observed bluer colours, but slightly sub-solar metallicities.

In general the spectroscopy seems to confirm photometric results, but not always, and it is necessary to obtain a good spectral S/N in the region of the envelope to properly investigate the stellar populations there. A larger sample is also necessary to explore the different types of objects classed as cDs and their differing evolutionary histories. The new 6.5m telescope TSPM and the first generation instrumentation will be ideal to carry out such a project as the good S/N needed in the faint halo regions for both imaging and spectroscopy will be obtainable in a reasonable exposure time. Going by previous experience with 2m telescopes we will ask for 5–10 min total exposures in *gri* filters and 30 min total in *u* using Megacam, and carry out spectroscopy with Binospec ($R = 1000$) with up to ~ 3 hour total exposures for positions in the faintest parts of the envelope, lesser exposures for more central positions. The observed colours and Lick spectral indices will be used with several stellar evolution codes to obtain the stellar populations in each position in the galaxy.

We have also carried out analysis in 2 dimensions of galaxy profiles using GALFIT to fit components to the underlying galaxy and envelopes. The main result so far is that the extended halo component frequently has a Sérsic index of close to 1, i.e. an exponential fall off with radius, similar to the results of Donzelli et al. (2011). We will extend this project considerably with the new imaging data from Megacam. The shape and Sérsic index of the halo component will influence the modelling of the formation and subsequent evolution of this component.

References

Ascaso, B.; Lemaux, B. C.; Lubin, L. M.; Gal, R. R.; Kocevski, D. D.; Rumbaugh, N.; Squires, G. 2014, *MNRAS*. 442, 589

Cooper, Andrew P.; Gao, Liang; Guo, Qi; Frenk, Carlos S.; Jenkins, Adrian; Springel, Volker; White, Simon D. M. *arXiv*, 1407.5627

Donzelli, C. J.; Muriel, H. & Madrid, J. P. *ApJS*, 195, 15

Fabian, A.C., Nulsen, P.E.J., & Canizares, C.R. 1982, *MNRAS*, 201, 933

Gallagher, J.S., & Ostriker, J.P. 1972, *AJ*, 77, 288

Kemp, S.N., Guzmán Jiménez, V., Ramírez Beraud, P., et al. 2009, *New Quests in Stellar Astrophysics II: Ultraviolet Properties of Evolved Stellar Populations*, Springer, 91

Merritt, D. 1984, *ApJ*, 276, 26

Neistein, E., van den Bosch, F.C. & Dekel, A. *MNRAS*, 372, 933

Oemler, A. Jr. 1976, *ApJ*, 209, 693

Pérez-Hernández, E. 2014, *Espectroscopía de Halos de Galaxias tipo cD's*, Undergraduate thesis, University of Guadalajara

Schombert, J.M. 1988, *ApJ*, 328, 475

The Butcher-Oemler Effect: Quenching vs. Ignition: A Scientific Case for TSPM and MMT

Omar López-Cruz and Héctor Javier Ibarra Medel

Instituto Nacional de Astrofísica, Óptica y Electrónica
Luis Enrique Erro 1, Tonantzintla, Puebla, México

Potential instrumentation: Megacam + Binospec

1 Motivation

The Butcher-Oemler effect (e.g., Butcher & Oemler 1978, 1985) has been debated for a long time (e.g., Pimbblet 2003), There are remaining issues awaiting to be explained in order to understand the gradual increment with redshift of blue galaxies in the core of rich clusters of galaxies. It is still unclear, if cluster galaxies at high redshifts are bluer because of the detonation of starburst (ignition) or the shutting-off of stellar formation (quenching).

The galaxies shutoff of star formation is one of the most important features in the understanding the galaxy evolution. There is no universal mechanism that explains quenching (Tal et al. 2014; Slater & Bell 2014); rather, exists multiple theories that can explain the observed quenching (e.g., Lin & Faber 1983; Dekel & Silk 1986; Efstathiou 1992; Birnboim & Dekel 2003; Di Matteo et al. 2005). However, it has been suggested that environmental and local properties can stimulate an specified quenching mechanism (Tal et al. 2014). For example, for low mass galaxies, process like ram-pressure, strangulation, and harassment (environmental conditions) can be used to explain the shutoff of star formation by driving cold gas away (e.g., Gunn & Gott 1972; Larson et al. 1980; Farouki & Shapiro 1981; Tal et al. 2014). Also, local galaxy properties can activate the quenching by heating up the galaxy gas (Guo 2014; Tal et al. 2014). These process can be originated by AGN feedback (e.g., Kauffmann et al. 2004; Bower et al. 2006; Guo 2014), strong virial shocks in halos (the halo quenching model, Birnboim & Dekel 2003; Dekel & Birnboim 2006), quasar activity (that will generate outflows that deplete the gas content in galaxies, Sanders et al. 1988; Di Matteo et al. 2005), cosmological starvation (in massive galaxies, e.g., Feldmann & Mayer 2015), or stellar feedback. Whatever process domains, it is directly dependent with the galaxy mass (Woo et al. 2013).

In addition, cluster galaxies can be divided in two categories, satellite galaxies and central galaxies. The central galaxies are the most massive galaxies of a clustered system, and usually reside in the potential center of their systems. Satellite galaxies are the remaining galaxies that surrounds central galaxies, typically with eccentric orbits (van den Bosch et

al. 1999). According with the sub-halo mass function, masses of satellite galaxies are much lower than central galaxies (Giocoli et al. 2008; Boylan-Kolchin et al. 2010). Therefore, the quenching in satellite galaxies are more susceptible to be activated from environmental conditions ("environmental quenching", e.g, Peng et al. 2010, 2012; Woo et al. 2013; Tal et al. 2014). In contrasts, the quenching efficiency for central galaxies is given by local factors that directly depends on their masses ("mass quenching", e.g., Birnboim & Dekel 2003; Peng et al. 2010; Woo et al. 2013; Guo 2014; Feldmann & Mayer 2015). In fact, it is observationally known that central galaxies suffer a star formation quenching when their halo masses reach a specific mass cut (Brammer et al. 2011; Tal et al. 2014). In addition, observations of Local Group dwarf galaxies and satellite galaxies have demonstrated that there is a mass dependence with their quenching efficiency, where galaxies with lower masses present a higher quenching fraction (Wetzel et al. 2013; Slater & Bell 2014).

Therefore, the star formation efficiency in quiescent galaxies also directly depends on their total dark halo masses (e.g., Peng et al. 2010; Woo et al. 2013; Feldmann & Mayer 2015). This is clearly seen in the relative stellar mass versus halo mass relationship (SMHR), that have a star formation efficiency peak around $10^{11} \mathcal{M}_\odot$ (e.g., Yang et al. 2012; Leauthaud et al. 2012; Behroozi et al. 2013; Woo et al. 2013; Tal et al. 2014). This relationship represents the transition function between the theoretical halo mass function and the observed stellar mass function (e.g, Vale & Ostriker 2006; Rodríguez-Puebla et al. 2012; Yang et al. 2012). This connection was proved by the application of abundance matching techniques (AMTs, Vale & Ostriker 2006) that relate theoretical halo masses with observed galaxy luminosities or masses. This technique consists to match the observed galaxy abundances, with the expected abundances from a cumulative theoretical halo mass function. In addition, since dark halos of satellite galaxies suffer tidal disruptions more severely than massive galaxies due to their low gravitational potentials; then, it is expected that the mass profiles of their stellar bodies suffer the same tidal stripping as their host dark matter halo profiles (Arnaboldi 2014). On the other hand, quenched central galaxies continue growth their masses via mergers. Therefore, it is expected that the dark matter halo profiles of central galaxies differ from their stellar mass profiles. Hence, dynamical evolution of cluster galaxies and their interaction among their galaxy companions creates a dependence with the truncation of their mass profiles.

The study of the evolution of the quenching efficiency along a big mass range (from dwarfs satellite to big central galaxies) will characterize the evolution of the SMHR. This characterization not only retrieves important constraints to some cosmological models (since it fixes the actual halo mass function), but also indicates the evolution of the stellar mass function, and retrieves the co-evolution of the host dark matter halo profiles with their inner stellar bodies.

2 Proposed Observations

Hence, we want to characterize the SMHR and its evolution by studying the star formation process in quiescent galaxies in high-density environments. To achieve this aim, we propose to observe a sample of about 30 rich clusters of galaxies, selected from optical (e.g., Gilbank et al. 2011) and by the Sunyaev-Zeldovich effect (SZE) signal (Planck Collaboration et al. 2014). The selected clusters should be in the range $0.3 \leq z \leq 0.7$. Cluster galaxies should be sampled down to $M^\star + 2$ mag, within the first turn-around radius (e.g., Tully 2015; Ibarra-Medel 2015). TSPM+Megacam in two bands for object selection, and weak lensing

analysis, follow-up observations with TSPM+BINOSPEC will allow us to determine cluster membership and to measure galaxy properties. We are interested in galaxy masses, chemical evolution, and star formation rates. The scientific drivers of the proposed observations are as follows:

- To characterize the evolution of the dark matter halos from low mass to massive galaxies in clusters or groups by using observations and simulations.
- To estimate from a direct or indirect observation the baryonic and dark matter content of clustered galaxies.
- To perform a detailed study of the stellar populations in cluster galaxies and follow their star formation histories (SFH) and trace it dependance with radius.
- To study the quenching evolution and its dependence with their host galaxy halo mass using cosmological hydrodynamic simulations such as the Eris and Illustris simulation (Guedes et al. 2011; Vogelsberger et al. 2014b).

3 Analysis

Data from this project will allow us to perform a detailed study of the matter content and their quenching in cluster galaxies by using high-performance techniques such as gravitational lensing techniques, scaling laws (SLs), caustic techniques (phase space diagrams, e.g., Kaiser 1987; Regos & Geller 1989; Diaferio & Geller 1997), and stellar population synthesis. Therefore we can explore the kinematic, stellar and dark matter mass profiles of cluster galaxies in addition of their star formation activities from observational and simulated data.

3.1 Selection of Cluster Galaxies

To distinguish from field galaxies, whatever the data is from a simulation or observation, I will use spectroscopic data (or projected LOS galaxy velocity data) to perform multiple membership selection criteria, such as the 3σ algorithm (Yahil & Vidal 1977), rendering techniques (by overdensity selection, Ibarra-Medel et al. 2014), and caustic selection (see §3.2, below, and Serra et al. 2011; Alpaslan et al. 2012). The selection criterion based in the 3σ algorithm is an iterative selection process that retrieves a robust membership indicator. For each iteration, this approach estimates the average velocity and the velocity standard deviation for a galaxy sample. Hence, it is possible to define two velocity limits and selects all galaxies that lie within it. Therefore, once each iteration retakes, this procedure selects a new galaxy sub-sample. This process finishes when the velocity limits are the same as the immediate predecessor sub-sample. When the system converges, the background contribution must be zero. The iterative and convergence nature of this scheme provides robustness to the membership selection criterion. This process pretends to select galaxies that are gravitationally bounded to the cluster. Also, We have developed a cluster membership technique to look for galaxy numerical overdensities. In this cluster galaxy membership criterion, the algorithm selects the three-dimensional numerical overdensity region that encloses a virialized region. Therefore, galaxies within this region represent the members of a self-gravitational structure. This method can be employed to provide a selection criterion for observed galaxies from large

spectroscopic surveys and/or simulated galaxies from cosmological simulations. The method look for these overdensities using an adaptive method based on the Delaunay Tessellation Field Estimator (DTFE, Schaap & van de Weygaert 2000). The DTFE creates a continuous density field using a Delaunay tessellation, this tessellation uses all galaxy positions as their vertexes (e.g., Schaap 2007). Then, the sum over all tetrahedral volumes that are adjacent to a galaxy position is equivalent to the volume of the representative Voronoi cell of this galaxy (?Platen et al. 2011). Hence, the inverse of the volume of the representative Voronoi cell times 4 (the number of spatial dimensions plus one) returns the numerical density estimator at this galaxy position. This tool maps the three-dimensional shape of a cluster and its substructures without any other assumption than the selection of a density threshold. By using halo occupation distribution (HOD) models, the method selects a threshold that maps virialized structures. Therefore, galaxies selected within these three dimensional numerical density contours represent members of gravitationally bounded structures.

3.2 Analysis of Caustics

We also plan to use caustic techniques; these techniques can trace the dark matter component without assuming a virial equilibrium. The caustics represent the maximum velocity along the line-of-sight (LOS) that a galaxy (or star) can reach without escaping from a gravitationally bounded system (galaxy cluster or stellar system). Therefore, the relation between the escape-velocity and the caustics describes directly the potential profile of the system and therefore their total mass (Diaferio 1999). The caustic technique was employed by Serra et al. (2010) to compute the line-of-sight velocity dispersion profile for four dwarf spheroidal galaxies. Hence, with the use of SLs, lensing and caustic techniques, it is possible to constrain and/or recover a detailed profile of the dark matter content in galaxies and galaxy groups.

See Figure 1, where we show the application of the technique that we have developed to identified substructures, and determine masses through caustic analysis.

3.3 Weak Gravitaional Lensing

The high quality data from TSPM+Megacam will allow us to measure the deformation of background galaxies to estimate the cluster's dark matter distribution using the gravitational lensing technique. This technique uses the lens effect that is produced by massive objects, when their gravity bends the light path of foreground objects (Einstein 1936). Therefore, it is possible to model the amount of unseen dark matter that is needed to reproduce the observed shear (for week lensing) or bend (for strong lensing) on the shape of background galaxies. Hence, with the use of softwares that implement parametric methods and Bayesian statistics such as LENSTOOL (Kneib et al. 2011). With this study, we will be able to reconstruct the dark halos profiles using strong and week lensing techniques. In addition, we can use SLs to trace the dynamical mass within galaxies. These SLs assume that the galactic internal dynamics (σ or V), in association with the galactic scale (R), traces the dynamical galaxy mass ($\mathcal{M}_d$). Since the Mass-to-Light ratio ($\mathcal{M}/\mathcal{L}$) connects the light with its mass, the light of a galaxy also correlates with σ and/or R. For example, Faber & Jackson (1976) proposed a SL
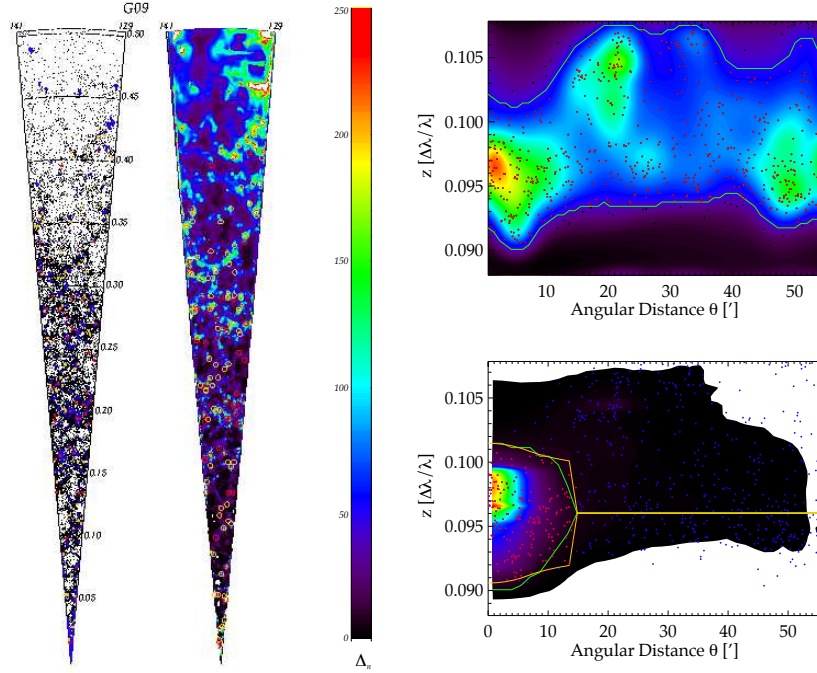
Fig. 1: Right: This figure depicts examples of the techniques that we have developed to study the galaxy distribution of GAMA fields G09 with its continuous overdensity field in cone plot diagrams (redshift vs right ascension). A similar analysis can be performed in the propose observations with TSPM+Megacam and follow-up observations with TSPM+BINOSPEC. The right panel shows color-coded overdensities according with the galaxy number overdensity value. In the cone plots, the yellow points and circles are the selected clusters using a sigma-clipping algorithm. The red points and circles are the clusters whose multiplicities are greater than 10. For the discrete galaxy distribution cone plots, the blue points are all the overdensity detections. Top-Left: Example of the application of the caustic method with substructures. Bottom-Left: The same case once we clean the substructure contribution. The colors represent the continuous galaxy number density normalized at the maximum density of the region. The blue points represent the galaxies on the redshift space and the red points are the galaxies located within the caustic curves. The yellow line is the final location of the caustic amplitude.

involving the luminosity and velocity dispersion in early-type galaxies. Furthermore, Tully & Fisher (1977) found the corresponding SL for spiral galaxies that relates the maximum rotational velocity of the disk with the luminosity of a galaxy. The Tully-Fisher and Faber-Jackson relationship was previously used by Geha et al. (2006) to estimate the mass content of extremely low-mass dwarf galaxies. On the other hand, SLs depends that galaxies being in a virial equilibrium (without any external gravitational perturbation) to be valid.

3.4 Stellar Populations

Spectra obtained with BINOSPEC will have enough resolution to study of stellar populations, stellar mass content, and quenched fraction in clustered galaxies, and AGN fraction. To achieve this aim, we plan to use the spectral stellar libraries of Bruzual & Charlot (2003) to perform a spectral energy distribution (SED) fit from observed galaxies. These libraries use a Salpeter stellar initial mass function (IMF), and return the values of single stellar populations for six metallicity values and 127 ages. Consequently, we will use stellar population synthesis codes (such as the STARLIGHT code, Cid Fernandes et al. 2005) that uses photometric magnitudes or spectral data to reconstruct the galaxy SED. In addition, galaxy spectra demand the use of aperture corrections, since fibers cover a physical and fixed size, generating a possible bias. On the other hand, it is possible avoid this bias by using photometric magnitudes that contains the 90% of the total galaxy flux to reconstruct the galaxy SED.

3.5 Confrontation of Models with Observations

Finally, we plan to use cosmological hydrodynamical simulations to study the quenching activation in central and satellite galaxies for low to high redshift. In the past year, the state of the art in cosmological simulations presents an alternative to studying the evolution of the dark matter in conjunction with their visible matter (e.g. the Illustris simulation, Vogelsberger et al. 2014a,b). Therefore, these type of simulations provide the perfect tool to explore the co-dependency between dark matter halos and their stellar mass contents. These type of studies return valuable information that complement the observational data of quenching galaxies. Also, these simulations provides information to understand the process of the observed quenching lag in satellite galaxies (Feldmann & Mayer 2015), the effects to take (or not to take) into o account AGN feedback, SMBHs, ram-pressure or other process that can suppress the star formation in quiescent galaxies.

4 Perspective

Galaxy evolution and its relation with the environment is a key issue in cosmology. TSMP and its host instrumentation will allow us to tackle galaxy evolution in rich clusters of galaxies at intermedia redshifts with unprecedented detailed. This observations may help to settle the quenching or ignition controversy, and as a corollary, the BOE.

References

Alpaslan, M., Robotham, A. S. G., Driver, S., et al. 2012, MNRAS, 3012
Arnaboldi, M. 2014, Astronomical Society of the Pacific Conference Series, 486, 16
Behroozi, P. S., Wechsler, R. H., & Conroy, C. 2013, ApJ, 770, 5
Birnboim, Y., & Dekel, A. 2003, MNRAS, 345, 349
Bower, R. G., Benson, A. J., Malbon, R., et al. 2006, MNRAS, 370, 645
Boylan-Kolchin, M., Springel, V., White, S. D. M., & Jenkins, A. 2010, MNRAS, 406, 896

Brammer, G. B., Whitaker, K. E., van Dokkum, P. G., et al. 2011, ApJ, 739, 24
Bruzual, G., & Charlot, S. 2003, MNRAS, 344, 1000
Butcher, H., & Oemler, A., Jr. 1978, ApJ, 226, 559
Butcher, H. R., & Oemler, A., Jr. 1985, ApJS, 57, 665
Cid Fernandes, R., Mateus, A., Sodré, L., Stasińska, G., & Gomes, J. M. 2005, MNRAS, 358, 363
Dekel, A., & Birnboim, Y. 2006, MNRAS, 368, 2
Dekel, A., & Silk, J. 1986, ApJ, 303, 39
Delaunay, 1934, B. Bull. Acad. Sci. URSS, VI, Classe Sci. Mat. pp 793-800
Diaferio, A., & Geller, M. J. 1997, ApJ, 481, 633
Diaferio, A. 1999, MNRAS, 309, 610
Di Matteo, T., Springel, V., & Hernquist, L. 2005, Nature, 433, 604
Driver, S. P., Hill, D. T., Kelvin, L. S., et al. 2011, MNRAS, 413, 971
Efstathiou, G. 1992, MNRAS, 256, 43P
Einstein, A. 1936, Science, 84, 506
Faber, S. M., & Jackson, R. E. 1976, ApJ, 204, 668
Farouki, R., & Shapiro, S. L. 1981, ApJ, 243, 32
Feldmann, R., & Mayer, L. 2015, MNRAS, 446, 1939
Geha, M., Blanton, M. R., Masjedi, M., & West, A. A. 2006, ApJ, 653, 240
Gilbank, D. G., Gladders, M. D., Yee, H. K. C., & Hsieh, B. C. 2011, AJ, 141, 94
Giocoli, C., Tormen, G., & van den Bosch, F. C. 2008, MNRAS, 386, 2135
Guedes, J., Callegari, S., Madau, P., & Mayer, L. 2011, ApJ, 742, 76
Guo, F. 2014, ApJ, 797, LL34
Gunn, J. E., & Gott, J. R., III 1972, ApJ, 176, 1
Ibarra-Medel, H. J., Lara-López, M., López-Cruz, O. & the GAMA team. 2014, arXiv:1410.0748
Hibarra-Medel, H. J. 2015, Ph.D. Tesis, INAOE.
Kaiser, N. 1987, MNRAS, 227, 1
Kauffmann, G., White, S. D. M., Heckman, T. M., et al. 2004, MNRAS, 353, 713
Kneib, J.-P., Bonnet, H., Golse, G., et al. 2011, Astrophysics Source Code Library, 1102.00
Larson, R. B., Tinsley, B. M., & Caldwell, C. N. 1980, ApJ, 237, 692
Leauthaud, A., Tinker, J., Bundy, K., et al. 2012, ApJ, 744, 159
Lin, D. N. C., & Faber, S. M. 1983, ApJ, 266, L21
Peng, Y.-j., Lilly, S. J., Kovač, K., et al. 2010, ApJ, 721, 19
Peng, Y.-j., Lilly, S. J., Renzini, A., & Carollo, M. 2012, ApJ, 757, 4
Pimbblet, K. A. 2003, PASA, 20, 294
Planck Collaboration, Ade, P. A. R., Aghanim, N., et al. 2014, A&A, 571, AA29
Platen, E., van de Weygaert, R., Jones, B. J. T., Vegter, G., & Calvo, M. A. A. 2011, MNRAS, 416, 2494
Regos, E., & Geller, M. J. 1989, AJ, 98, 755
Rodríguez-Puebla, A., Drory, N., & Avila-Reese, V. 2012, ApJ, 756, 2
Tal, T., Dekel, A., Oesch, P., et al. 2014, ApJ, 789, 164
Tully, R. B., & Fisher, J. R. 1977, A&A, 54, 661
Salpeter, E. E. 1955, ApJ, 121, 161
Sanders, D. B., Soifer, B. T., Elias, J. H., et al. 1988, ApJ, 325, 74
Schaap, W. E. 2007, Ph.D. Thesis,
Schaap, W. E., & van de Weygaert, R. 2000, A&A, 363, L29
Serra, A. L., Diaferio, A., Murante, G., & Borgani, S. 2011, MNRAS, 412, 800
Serra, A. L., Angus, G. W., & Diaferio, A. 2010, A&A, 524, A16
Slater, C. T., & Bell, E. F. 2014, ApJ, 792, 141
Tully, R. B. 2015, AJ, 149, 54
Vale, A., & Ostriker, J. P. 2006, MNRAS, 371, 1173
van den Bosch, F. C., Lewis, G. F., Lake, G., & Stadel, J. 1999, ApJ, 515, 50
Vogelsberger, M., Genel, S., Springel, V., et al. 2014b, MNRAS, 444, 1518
Vogelsberger, M., Genel, S., Springel, V., et al. 2014a, Nature, 509, 177
Wetzel, A. R., Tinker, J. L., Conroy, C., & van den Bosch, F. C. 2013, MNRAS, 432, 33
Woo, J., Dekel, A., et al. 2013, MNRAS, 428, 3306
Yahil, A., & Vidal, N. V. 1977, ApJ, 214, 347
Yang, X., Mo, H. J., et al. 2012, ApJ, 752, 41

Part IV
Future Instrumentation

Wide-field imaging Fourier transform spectroscopy: a second generation instrumentation proposal for the TSPM

F. Fabián Rosales-Ortega[1], Edgar Castillo[1], Sebastián F. Sánchez, Jesús González[2], Salvador Cuevas[2], Miguel Chávez[1], et al.

[1]*Instituto Nacional de Astrofísica, Óptica y Electrónica*
Luis Enrique Erro 1, Tonantzintla, Puebla, México

[2]*Instituto de Astronomía, IA-CU, Universidad Nacional Autónoma de México*
Circuito de la Investigación Científica s/n, Ciudad Universitaria, Del. Coyoacán, C.P. 04510, México, D.F.

Abstract

Many physical processes in astronomy are still hampered by the lack of spatial and spectral resolution, and also restricted to the field-of-view (FoV) of current 2D spectroscopy instruments available worldwide. It is due to that that many of the ongoing or proposed studies are based on large-scale imaging and/or spectroscopic surveys. Under this philosophy, large aperture telescopes are devoted to the study of intrinsically faint and/or distance objects, covering small FoVs, with high spatial resolution, while smaller telescopes are devoted to wide-field explorations. The future astronomical surveys, however, should be addressed by acquiring un-biases, spatially resolved, high-quality spectroscopic information for a wide FoV. Therefore, we aim to explore a possible instrument for the future 6.5m Telescopio San Pedro Mártir (TSPM), that would provide un-biased wide-field (few arcmin) spectroscopic information, with the flexibility of operating at different spectral resolutions ($R \sim 1 - 20000$), with a spatial resolution limited by the atmosphere (seeing), and thus to be used in a wide range of astronomical problems. This instrument would make use of the Fourier Transform Spectroscopic technique, which has been proved to be feasible in the optical wavelength range (350-1000 nm) with designs such as SITELLE (CFHT). The proposed instrument would be designed for and installed in the future 6.5m TSPM, based on the experience acquired during the development and integration of a similar prototype instrument being currently built at INAOE for the 2.1m telescope at the Observatorio Astrofísico Guillermo Haro (OAGH) in Cananea, Mexico. We describe here the basic technical description of a Fourier transform spectrograph with important modifications from previous astronomical versions, as well as the technical advantages and weakness, and the science cases in which such an instrument can be implemented.

1 Introduction

There are basically two traditional approaches to obtaining spectral information on extended astrophysical objects: narrow-band imagery and integral field dispersive spectroscopy. Imagery with filters allows the observer to map a target in selected wavelength ranges and to extract the required physical information by comparing the relative flux of the sources in these bands. Images of the targets in the different band passes must be obtained one after the other with a CCD detector, rejecting each time all photons excluded by the selected filters (up to 99.8%). Moreover, narrow-band imagery does not provide a high enough spectral resolution to determine kinematic information.

Dispersive spectroscopy with slits allows a much finer spectral resolution at the expense of spatial information on the targets. Extensively used since the mid-19th century to obtain the spectrum of individual stars or small slices of extended objects, dispersive spectroscopy has been transformed by the advent of multi-object spectrographs (MOS)) in the 1990's: multiple slitlets or optical fibers are positioned at the location of the targets in a wide field of view (FoV), the light of which is then sent to a disperser and recorded on a CCD (e.g. 2dF, Colles et al. 2001). Major breakthroughs have also been obtained in astronomical instrumentation over the last decade by combining imagery and spectroscopy into a single experimental observation technique that produces cubes of data, which is typically referred as 2D spectroscopy. This technique has revolutionized data collection by allowing to obtain spectra of a large number of objects dispersed in a large field using deployable fibres or to spatially sample relatively small (few arcsec) objects using integral field units or IFU (e.g. GMOS, Allington-Smith et al. 2002; SAURON, Bacon et al. 2001; PINGS, Rosales-Ortega et al. 2010; CALIFA, Sánchez et al. 2012). However, the vast majority of imaging spectrometers used on telescope to date are build on dispersive approaches which must sacrifice detector pixels to retrieve the spectral content instead of scene elements. Given the limitations of modern array detectors, different instrument concepts convey different trades that each enhances the possibility of discovery for a given science program category.

Nonetheless, the ongoing and planned 2D spectroscopy surveys in the coming decade are motivated by some of the most compelling questions on stars, Galaxy/galaxy formation, evolution and cosmology. There is an acute need for large-scale surveys in both hemispheres with wide-field, highly-multiplexed spectrographs. Several 2D spectroscopy survey instruments are already in rapid development around the world, and are anticipated to be in use well before the end of this decade. These include complex single and multi-object IFUs for mapping individual galaxies, as well as a new generation single-fiber MOS instruments devised to obtain thousands of integrated galaxy spectra, some even extending into the near IR.

On the other hand, given the worldwide trends in the use of astronomical infrastructure, in the forthcoming decades large aperture telescopes ($>$20m) will be devoted to the study of intrinsically faint and/or distance objects, covering small FoVs, with high spatial resolution, while smaller telescopes ($<$8m) will be devoted to wide-field explorations. In this context, one can speculate about the most efficient use of 2-6m class telescopes worldwide (including the TSPM) and their related instruments in 10-15 years, as they would need to neccesarily find synergies with the new generation of large telescopes both ground-based and space ones. One possibility might be by conceiving an instrument that, within a reasonable budget, could be capable of acquiring un-biased, spatially resolved, high-quality spectroscopic information for really wide FoVs (10-30 arcmin). Such telescope-instrument binomial would represent a
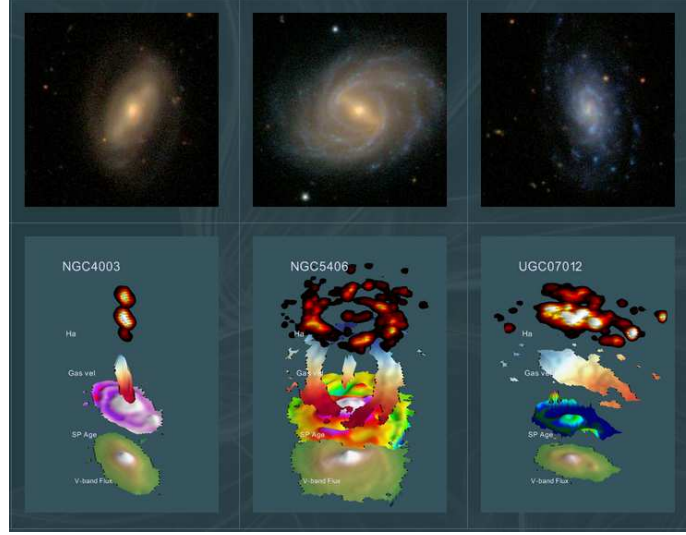
Fig. 1: Example of galaxies observed as part of the CALIFA survey based on the integral field spectroscopy (IFS) technique. The top-row shows RGB composite images from SDSS. The bottom-row shows observables derived from the IFS datacubes, from bottom to top: V-band flux, stellar populations age map, gas velocity and Hα emission maps (figure adapted from Sánchez et al. 2012).

natural complement to the new generation of ground and space telescopes in the next decades, and would set a milestone in the history of observational astronomy. Such binomials would impact in large number of research programs and scientific cases, and will naturally extend to numerous other areas of broad community interest, setting a transformational era that will certainly help to unravel many of the fundamental puzzles of contemporary astrophysics.

2 Beyond MOS and fibres: wide-FoV, high-spatial resolution spectroscopy

In the extragalactic context, the CALIFA, SAURON and ATLAS^{3D} (Cappellari et al. 2011) surveys represent the benchmark for current and future 2D spectroscopy surveys on nearby galaxies (see Fig. 1). MaNGA (Drory et al. 2015) and SAMI (Croom et al. 2012) will observe thousands of galaxies using IFS, providing important statistical information (although with a coarse spatial resolution), while MUSE (Bacon et al. 2004) will become the most powerful IFS, seeing-limited instrument in the world. However, many physical processes in astronomy are still hampered by the lack of spatial and spectral resolution. As shown by Mast et al. (2014), there can be an important information loss due to spatial resolution degradation of IFS surveys at different redshifts. It is worth noting that the important figure of merit is the ratio between the spaxel size and the typical scale-length at a certain redshift. The loss of information due to spatial degradation might cause an incorrect interpretation of common ob-
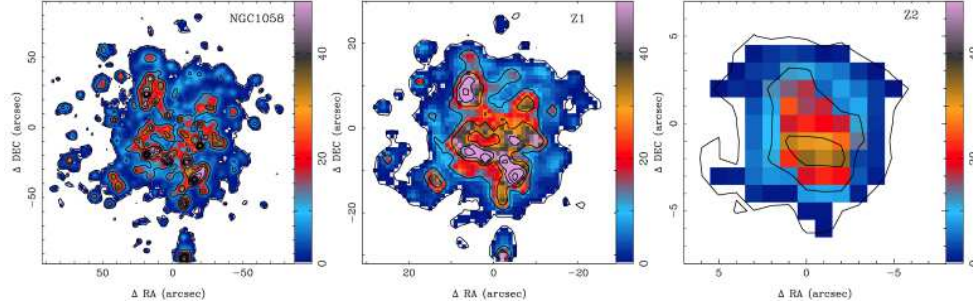
Fig. 2: Left: IFS Ha image of NGC1058 from the PINGS sample. Middle-Right: simulated IFS observations of NGC1058 at different redshifts, Z1 associated with the CALIFA survey (z 0.02) and Z2 with an hypothetical higher redshift survey, e.g. SAMI 1.6"/fibre, or MaNGA 3"/fibre (figure adapted from Mast et al. 2014).

servables in the considered framework. The spectroscopic blending of local structures might not result in global trends or averaged values, as shown in Fig. 2 and Fig. 3.

As mentioned before, current 2D instrument/survey concepts convey different trades for a particular science program. The vast majority of spectrometers are based on dispersive approaches that must *sacrifice* detector pixels to retrieve the spectral content instead of scene elements. A revolutionary approach would consist in an instrument capable of simultaneously obtaining spatially resolved spectra on extended areas (few arcmin) with a 100% filling factor, with a spatial resolution limited by the atmosphere (seeing), and a flexible spectral resolution (up to $R \sim 10^4$) over a wide spectral range in a mid-class (4-8m) telescope. Nowadays, the only instrument based on a dispersive approach with such capabilities is (the complex and largely expensive) MUSE-VLT spectrograph (see Fig. 4). Therefore, if one wants to devise wide-FoV, high spatial resolution 2D spectroscopy instruments within a reasonable budget, new technologies have to be sought. The technique known as imaging Fourier transform spectroscopy (IFTS) is very promising on that regard.

2.1 The IFTS concept

An astronomical imaging Fourier transform spectrometer (IFTS) is basically a Michelson interferometer inserted into the collimated beam of an astronomical camera system. Contrary to conventional integral field dispersive spectrographs, all detector pixels are used for imagery as with the Fabry-Pérot, but instead of acquiring spectral slices one by one (thus rejecting every other wavelength) to cover the entire waveband of interest, an "all in one" approach is used. Likewise, all wavelengths from the field are simultaneously transmitted to either one or both of the interferometer outputs in which the array detectors sit. This configuration results in a large light gathering power since no light is lost except through items common to any optical design: substrate transmission, coatings efficiency, and quantum efficiency of the detectors.

Fig. 5 shows how a Fourier Transform Spectrometer works: the core of the instrument is a classical Michelson interferometer, the incoming beam from the telescope is first split
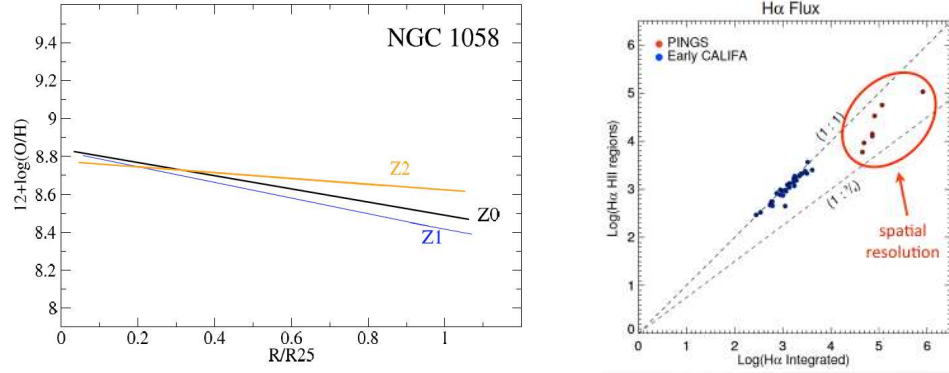
Fig. 3: Left: Linear regressions of the oxygen abundance gradient of NGC1058 for the three redshift regimes, note the wrong gradient derived for Z2 (see Fig. 1, figure adapted from Mast et al. 2014). Right: Comparison of Ha flux obtained from the integrated spectra of a sample of spiral galaxies to the sum of Ha flux of individual HII regions, the 1-to-1 correspondence disapears once the IFS observations have enough spatial resolution to discriminate difuse emission (Figure adapted from Castellanos-Durán et al. in prep).

into two equal parts by a beamsplitter. Half the light is transmitted through the beamsplitter, bounces back on a moving mirror and interferes, in the beamsplitter, with the other half-beam which has, in the meantime, been reflected by the beamsplitter to a fixed mirror and bounced back. Initially, the optical path travelled by the two beams is the same; we are at the Zero Path Difference (ZPD) position. The two beams are in perfect phase when they combine and the interference is completely constructive: the detector receives the sum of the two beams while none of the light goes back to the source. The moving mirror is then slightly displaced, creating small offset in optical paths between the beams. These are not in phase anymore, the interference is not entirely constructive and the detector receives a bit less light while the difference goes back to the source. Typical displacements vary between 175 nm and a few micrometers, depending on the wavelength range and the desired spectral resolution.

Eventually, after a sufficiently large mirror displacement, the interference will be totally destructive: no light will be recorded on the detector; the entire beam will go back to the source. In practice, an interferogram is obtained by first moving the mirror to a predetermined position away on one side of the ZPD, moved by equidistant steps to the same position on the other side of the ZPD. The original frequency, or wavelength, of the incoming light beam is thus recovered by calculating the Fourier transform of the time dependent signal recorded by the detector.

2.2 IFTS versus Dispersive Spectrographs

An IFTS has two advantages over any system feeding a dispersive slit. The first is that, because an IFTS builds up the datacube frame-by-frame, the total number of available datacube elements is an entire CCD times the number of samples. By comparison, on a slit system
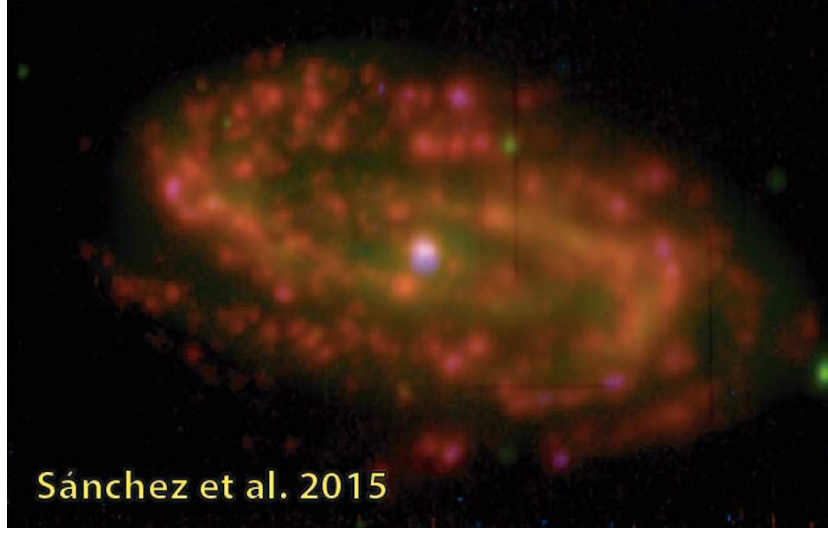
Fig. 4: True color image created from continuum subtracted narrow-band images of the IFS mosaic of NGC6754, illustrating the power of the combined large FoV and high spatial resolution of MUSE. The mosaic is composed of two ~ 1 arcmin pointings aligned east-west, with an overlapping area of ~ 16. Different seeing conditions for the for the East (~ 0.8) and for the West (~ 1.8) pointings are also clear. The final dataset comprises ~ 200k individual spectra. Each red structure corresponds to a single HII region.

the area of the slit limits the observed total angular area on the sky. Another way to look at this is that, for image slicers and fiber-fed spectrographs, all three dimensions of the datacube obtained are limited to a single CCD image. The other advantage of an IFTS is that the spectral resolution is flexible; it is not necessary to change gratings to "tune" the observing to the science or the observed object's faintness. The grating efficiency is analogously replaced by the modulation efficiency of the interferometer (see below) that would typically reach values higher than 80% over most of the instrument waveband.

2.3 IFTS versus Fabry-Pérot interferometer

The IFTS must be distinguished from filter systems including imaging Fabry-Pérot (FP) spectrographs or tunable filters. An IFTS accept all the light at all wavelengths. It only creates one interference between the two *branches* of a photon and records the phase difference. On the other hand, an FP creates multiple *branches* by multiple reflections inside a cavity creating constructive interferences only for a narrow band of wavelengths, rejecting most of the light. Also, the passband is periodic and one order has to be selected, liming the spectral range to a few angstroms. FP systems are better suited for narrow band observations of faint extended objects as they cut all the out-of-band noise to which IFTS would be sensitive. Moreover, on the spectral coverage, the Fabry-Pérot is considered more as a line profiler than a true spectrometer due to its limited spectral coverage.
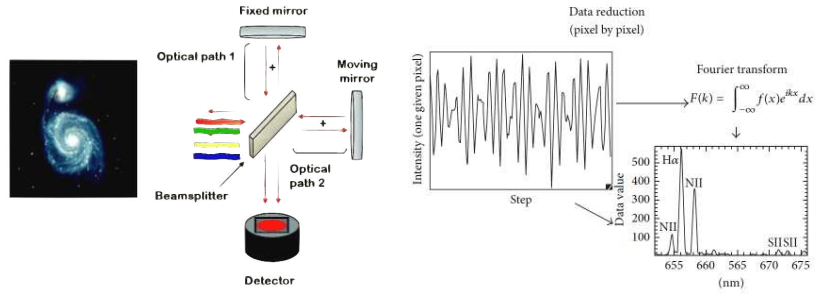
Fig. 5: Left: The Michelson interferometer consists of a beamsplitter used to separate the incoming beam into two equal parts, two mirrors on which the halves of the original beam are reflected back, a moving mechanism to adjust the position and orientation of one of the mirrors, and a metrology system (IR laser and detector) to monitor the mirror alignment. The result of an exposure is a data cube in the 3D space: R.A., Dec, Optical Path Difference (OPD). By scanning the OPD and taking images at every step, one gets a datacube composed of one interferogram for every pixel. Right: For a given pixel, the recorded intensity varies as a function of the OPD. An inverse Fourier transform of the signal produces a spectrum for every pixel in the image. The final result is a data cube in the 3D space: R.A., Dec, wavelength, with one spectrun per pixel of the detector, i.e. thousands of spectra per pointing. (Figures adapted from Drissen+ 2010, 2014).

2.4 IFTS drawbacks

The light gathering power of the IFTS is unsurpassed since it can almost be made to match the CCD performance in terms of waveband and FoV. Its optical design is similar to that of most focal reducers for astronomy, after considering the desired, science-driven, pixel sampling and total FOV, as well as field aberration. The design only has to allow a sufficient length of collimated beam space to insert the flat optics interferometer. The control of the chromatic aberration is however of greater challenge when compared to classical astronomical imaging cameras. This is because all wavelengths are imaged and sampled simultaneously as opposed to imaging with filters in which the telescope can be refocused to the central wavelength of the filter used. This can easily become a limiting factor for the spectral coverage of the instrument which otherwise is mostly limited by the beamsplitter efficiency band. The interferometer is then designed to prevent vignetting of the selected FoV and acts as a panchromatic modulator for each individual beam associated with every pixel. Calibration of the obtained data cubes is obviously pixel dependent and much care must be taken in this operation.

The greatest disadvantage of the IFTS is the difficulty of observing fluctuating sources Since an FTS inherently uses time domain multiplexing of the spectral data, with spectral intensity vs. modulation frequency translated into spectral intensity vs. wavenumber, any significant temporal fluctuations in the observed light intensity within the frequency range corresponding to the spectral features of interest represents noise in the derived spectrum. Furthermore, periodic fluctuations produce line shifts of the observed spectral features, with the implication that it is very difficult, for example, to measure AC modulated calibration sources. Under certain circumstances however, this aspect of an IFTS may be used to advan-

tage. For example, it is possible to use the broadening of ordinarily narrow spectral features as a measure of the degree of temporal fluctuation of the source term, and this can be used to distinguish transient or erratic spectral features.

2.5 Technical challenges in the construction of an IFTS system

As any professional optical instrument, an IFTS must include high-quality optics that allows a higher transmitance in the considered working wavelength. The performance of an IFTS is characterised by the modulation efficiency (ME), i.e. the capacity of the interferometer to modulate incident light, defined as:

$$ME = \frac{I(\text{modulated light})}{I(\text{incident light})}$$

.

The ME can be seen as the analog of difraction grating efficiency in dispersive spectrographs. The ME depends upon several factors, the most demanding from the technical point of view being:

- The surfaces qualitity of the optical components of the interferometer (mirrors, beamsplitter, etc.) at a given wavelength. The less optical quality, the less ME. One has also to consider the number of reflections within the instrument. It is required a surface optical quality (peak-to-valley) greater than $\lambda/20$.
- Alignment of the moving mirror and stability of the OPD during an exposure, which highly depend on the quality of the metrology system, the most important challenge for an IFTS system in the optical range. Any tiny variation in any direction, angle or alignment of the mirrors, would reduce the spatial coherence (interference) between the two recombined beams, effect which is more problematic at shorter (bluer) wavelenghts. The system requires monitoring the distance and aligment of the components several thousand times per second, combined with a fast correction by the use of actuators.

An additional factor is the CCD readout time. Given, that an interferogram is acquired through a series of hundreads of short exposures, the requiered time to read the CCD limits the global efficiency of the instrument, and thus the system requires a fast, low-noise readout CCD ($\sim$ 2s.) Nonetheless, the IFTS technique has been proved to be feasible in the optical wavelength range (350-1000 nm) with designs such as SpIOMM (Grandmont et al. 2003) and SITELLE (Drissen et al. 2010, currently under commissioning at CFHT), by using appropriate optical configurations, fast readout CCD detectors, and especially improved metrology and control systems.

Main advantages of an IFTS system

- A large FoV with a complete (100%) covering factor.
- Flexible spectral resolution ($R = 1 - 10^4$), easily tuned (optimal for $R \sim 2000$).
- Full optical wavelength coverage.
- Angular resolution limited by seeing.
- No diffuse light.

- Better precision in wavelength calibration (laser metrology system).
- High throughput, superb efficiency.

An IFTS is most efficient for:

- Low spectral resolution ($R \sim 100$) of very large FoV and/or crowded fields
- Moderate resolution ($R \sim 2000$) of extended sources
- High resolution ($R > 10000$) for extended, nearby, bright objects
- Large number of relatively bright objects in the FoV

Drawbacks

- Not suitable for for low SB objects (high spectral resolution modes)
- Control of chromatic aberration (high quality optics)
- Very precise mechanical scanning (flexures)
- Pixel-by-pixel calibration

3 Science with an IFTS instrument and a wide-FoV 6.5m class telescope (TSPM)

The current large-format astronomical surveys (e.g. SDSS, 2dF) provide multi-wavelength imaging on very broad fields, which are then combined with spectroscopic observations of a previously selected, magnitude-limited targets. Given the large amount of information that they provide, these surveys have contributed enormously to the development of modern astrophysics, however the present several restrictions. The most important being that the spectral information is restricted to a specific spatial region of the target, in the case of galaxies normally the central one (covered by the fibre), which prevents the study of properties that show a spatial variation (e.g. chemical abundances in spiral galaxies, dust properties, metallicity and age gradients of the stellar populations, etc.). This combined with the impossibility of covering spectroscopically a large number of targets given the limited number of fibres and spectrographs in a given instrument.

Two-dimensional spectroscopy came to revolutionize the field by allowing the spectroscopic observation of spatially-resolved objects. However, in general, this method offers a very short FoV (< 1 arcmin) with poor spatial and spectral resolution, which hampers the possibility to observe a large number of targets. That is why an IFTS would be the ideal instrument in case the target occupies a large fraction of the FoV of the instrument, or if one requires observing a large number of sources in a crowded FoV. The niche of opportunity of an astronomical IFTS is thus covering a very large FoV, with a spatial resolution limited by seeing), with a flexible, moderate-to-high spectral resolution ($R \sim 2000 - 10000$) and a wide spectral range coverage.
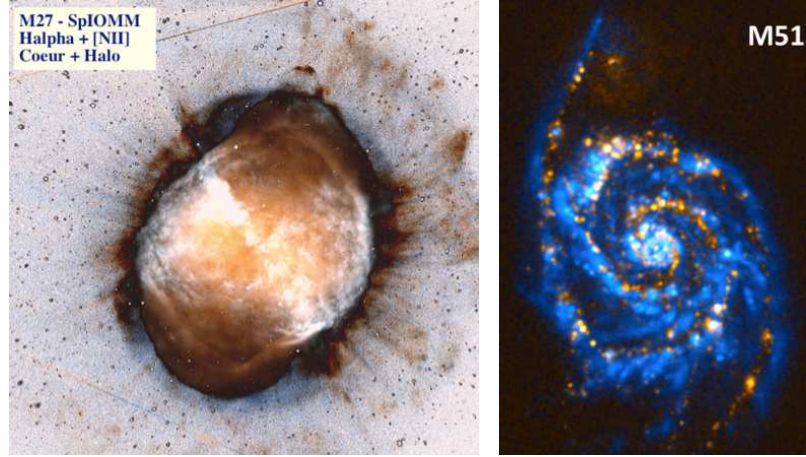
Fig. 6: Left: Hα + [NII] emission line combined image of the planetary nebula M27 obtained with the IFTS prototype SpOIMM. Right: False colour image of the nearby galaxy M51 showing in blue the Hα emission obtained by the SpOIMM IFTS prototype and in orange the NUV emission from the GALEX space telescope. Figures adapted from Drissen et al. 2008.

The potential scientific cases to be exploded by an IFTS instrument in the optical wavelength range are the following:

- **Evolution of cluster of galaxies.** The large FoV of an IFTS would allow to cover spatial regions corresponding to the virial radius of nearby clusters ($z < 0.04$) in reasonable observing times (0.25 to 1 degree FoV). The potential of an IFTS is perfect considering the high density of galaxies in the central regions of clusters, which would provide great statistics considering the large number of objects in such fields. Observations with an IFTS would allow to detect spectroscopically tidal and other environmentally features which are common in these dense environments and that can shed light on the physical processes governing the evolution of cluster galaxies.
- **Structure of Galactic HII regions.** Photoionized nebulae are essential to determine the chemical composition of the interstellar medium in galaxies, including the primordial helium abundance. Linked to this problem is the existence of abundance discrepancy problem measured through collisionally excited lines (CEL) or recombination lines (RL). The large FoV offered by the IFTS the best opportunity for obtaining the required spectral information of nearby Galactic HII regions with a complete spatial coverage, as well as the study of the impact of shock fronts originating from massive stelllar winds and the kinematics of HII regions.
- **Nebulae around evolved stars.** A meaningful link between local heavy element enrichment and the global chemical evolution of galaxies can only be established by detailed studies of individual windblown bubbles in our own galaxy. Winds of evolved stars, and their surrounding bubbles (planetary nebulae, luminous blue variables, Wolf Rayet ejects, supernovae remnants) are known to be globally enriched with products of nucleosynthesis. A complete survey of abundance, density, temperature and kinematic measurements in nebulae surrounding individual evolved stars or ionizing clusters, looking for non-homogeneities in the distribution of processed material (primarily nitrogen and oxygen),
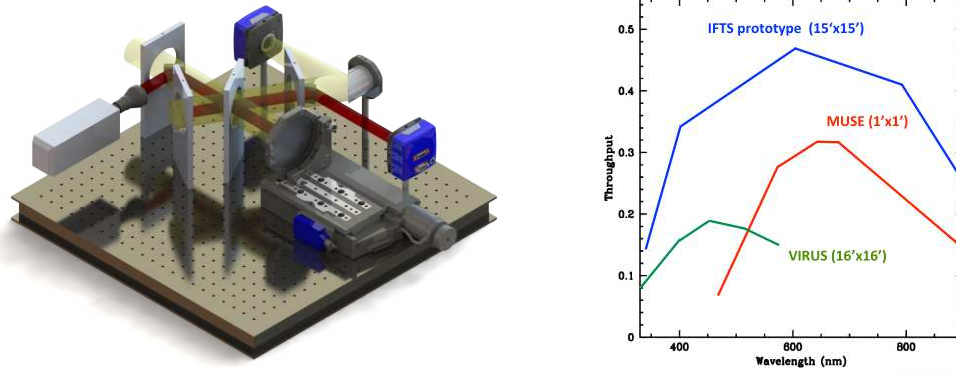
Fig. 7: 3D preliminary design render of the INAOE-IFTS prototype (PI F. Rosales-Ortega). There are two concentric beams, the red one is generated by an IR laser for metrology purposes and the yellow beam is the scientific collimated beam coming from the telescope. Right: Expected throughput of the IFTS prototype + telescope system as a function of wavelength for a 15×15 arcmin FoV (blue), compared to the MUSE (red) and VIRUS (green) spectrographs.

requires wide field spectroscopic mapping, and the IFTS will provide the required spatial and spectral coverage with the appropriate resolutions to perform such studies.

- **Nearby galaxies.** With its high efficiency and large field of view an IFTS will be the ideal instrument to study the chemical abundances, kinematics and stellar populations of nearby galaxies. Most of the conclusions drawn so far on the chemical evolution of galaxies are based on restricted or inhomogeneous data: galaxies studied with long-slit MOS or fiber-fed IFUs are restricted by their small FoV or a tiny fraction of the total surface of their targets. Fabry-Pérot or interference filter data usually cover a single line and so they are not able to produce line profiles and obtaining information through a wide spectral range. Thus, observations of large samples of nearby galaxies with the IFTS will revolutionize the study of galaxy chemical evolution.
- **Galaxies across the Universe.** Because the IFTS can be used without predefined filter in the whole visible waveband, they can be extremely useful to study the intermediate- to-high-z Universe in a relatively unbiased way. As an example, the IFTS will allow detection of Lyman-α emission in objects at $2 < z < 7$. The IFTS will sample the redshift space uniformly on a wide field allowing spectroscopic redshift determination and line profile analysis of many galaxies in a single observation.
- **Properties of open stellar clusters.** Although hundreds of open clusters are known in the Galaxy, only for very few of them their main properties (size, distance and reddening) have been estimated. The angular extension of the cluster (of the order of 1deg in some cases) is a limitation for obtaining spectroscopic data of a very large number of stars, and in cases of important crowding, the multi-fiber or multi-slit spectroscopy are not able to observe all the objects in the field at once. Again, an IFTS will allow obtaining spectroscopic information on crowded stellar clusters with complete spatial coverage.

Therefore the required parameters for the IFTS are the following:

- *Field of View of 15-30 arcmin circular.* This field of view will allow mapping in a single exposure most galaxy groups in the local Universe and in few exposures most galaxy clusters (up to $z = 0.02$). In addition, this will allow studying in close detail nearby galaxies with very high spatial resolution.
- *Spectral range from* $360 - 1000$ *nm.* The lower limit is imposed by the importance of detecting the [OII] 372.7,3.729 nm doublet for studies of galaxy evolution. The upper limit will be imposed by the decreasing of the total throughput of the system (optics + CCD) at near IR wavelengths. In any case, most of the emission and absorption lines of interest for galactic structure and evolution at optical wavelengths will be covered. F this reason the optics and CCD of IFTS will be optimized for optical wavelengths, and this naturally imposes the upper wavelength limit at 1 micron. The required lower limit in λ implies that the minimum OPD sampling must be $\Delta x = 180$ nm.
- *Resolving Power* $1 < R < 20000$. The spectral resolution of an IFTS is a function of the field of view as well as of the total OPD sampled. In this case, the desired field of view of 15-30 arcmin is this last factor the one that limits the spectral resolution. For most scientific cases (as the ones explained above) $R = 20000$ is largely enough at any wavelength in the allowed spectral range. For a resolving power $R = 20000$ at 650 nm the total scanned OPD would be of 7.8 mm.

4 A second-generation instrument proposal for TSPM

Throughout this document, we have presented the IFTS concept as a viable approach to integral field spectroscopy. A working IFTS instrument would combine high-resolution imagery and spectroscopy at levels unmatched by any other astronomical instrument. Such instrument would acquire spectra within images that are between 100 and 1000 times larger than is possible with conventional spectrographs. The science niche for the IFTS approach must take into account its main advantages (very wide field of view, high throughput, seeing-limited image quality, and flexible spectral resolution) and disadvantages (spectrally distributed noise, and necessary compromise between spectral coverage and resolution.

Given this niche of opportunity, we intend to build at INAOE-Mexico a pilot instrument based on the IFTS concept designed for and tested at the 2.1m telescope of the Observatorio Astrofísico Guillermo Haro (OAGH) in Cananea, that will provide un-biased wide-field (15 arcmin) spectroscopic information, with a spatial resolution limited by seeing (~ 1.4 arcsec), and flexible spectral resolution ($R \sim 500 - 2000$). The cost of this commercial prototype is about 250k USD. A proposal for this instrument has been officially submitted to the Mexican Council for Science and Technology (CONACyT).

The development process of this pilot instrument would allow us to understand the technical issues of this technology, interpret the data, prepare the reduction and analysis pipelines, train students and postdocs in the use of the data, and address a set of suitable astronomical problems. The experience acquired during the design, integration and testing of this prototype would be of paramount importance in order to explore a potential, second generation IFTS instrument for the future Telescopio San Pedro Mártir (TSPM) in Mexico. The ability to provide high spectral resolution across a large area of space will provide Mexican astronomers with a considerably larger data set an in a fraction of the time currently possible. An IFTS instrument could collect the same amount of data in a single night that would require weeks of
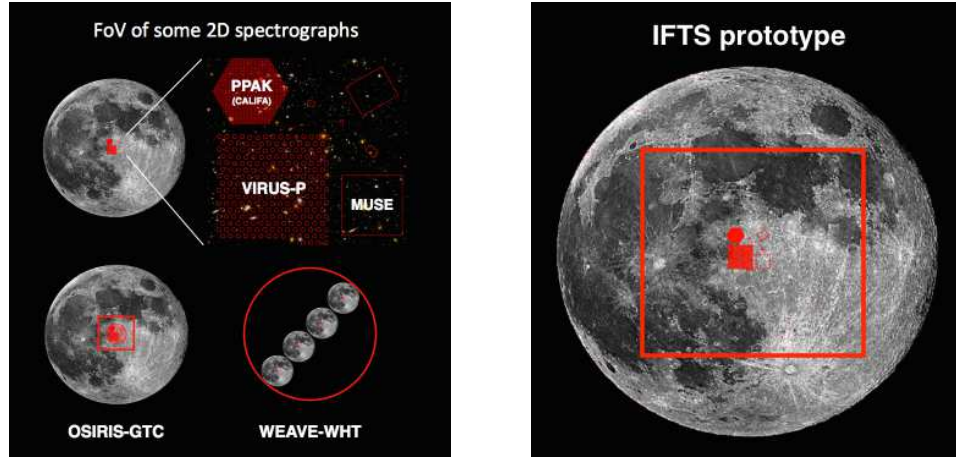
Fig. 8: Left: Field-of-View of some 2D spectrographs compared to the angular size of the Moon (30 arcmin). Bottom-left: The red square/circle represent the nominal (7 arcmin) and usable (3 arcmin) FoV of the OSIRIS-GTC tunable filter instrument respectively, compared to the size of the Moon. The FoV of the OSIRIS-GTC MOS is 2 arcmin, with a very limited spectral coverage. Bottom-right: the 2° FoV of the WEAVE-WHT instrument in which 1000 low spatial resolution fibres (1.3-2.6 arcsec) can be positioned, with low effective coverage. Right: Comparison of the 15 arcmin FoV for the proposed IFTS instrument for the 2.1m OAGH telescope to the angular size of the Moon (see main text).

observations with a conventional instrument, i.e. a huge improvement for telescope efficiency, where observing time is a scare resource, often restricted to few hours per project.

The arrival of such an instrument to the 6.5m-class TSPM, under exceptional skies, could mark a milestone in the astronomical observing techniques, allowing for a wide variety of science projects, promoting the competitiveness of the TSPM, and positioning the Mexican astronomical infrastructure as a leading contender in the world arena.

References

Allington-Smith et al. 2002, PASP, 114, 892
Bacon et al. 2004, SPIE, 5492, 1145
Cappellari et al. 2011, MNRAS, 413, 813
Colless et al. 2001, MNRAS, 328, 1039
Croom et al. 2012, MNRAS, 421, 872
Drissen et al. 2010, SPIE, 7735, 77350B
Drissen et al. 2014, Advances in Astronomy, 293856
Grandmont et al. 2003, SPIE, 4842, 392
Rosales-Ortega et al. 2010, MNRAS, 405, 735
Sánchez et al. 2012, A&A, 538, 8
Sánchez et al. 2015, A&A, 573, A105